JBC Papers in Press. Published on July 25, 2016 as Manuscript M116.725069
The latest version is at http://www.jbc.org/cgi/doi/10.1074/jbc.M116.725069

The Import of Proteins into the Mitochondrion of *Toxoplasma gondii*

Giel G. van Dooren[‡1], Lee M. Yeoh[§], Boris Striepen[¶] and Geoffrey I. McFadden[§]

From the [‡]Research School of Biology, Australian National University, Canberra, ACT, 2601, Australia, the [§]School of BioSciences, University of Melbourne, Parkville, VIC, 3010, Australia, and the [¶]Department of Cellular Biology and Center for Tropical and Emerging Global Diseases, University of Georgia, Athens, GA, 30602,USA.

Key words: *Toxoplasma gondii*, parasite, mitochondria, protein import, intracellular trafficking

ABSTRACT

Outside of well-characterized model eukaryotes, there is relatively little known about the translocons that transport proteins across the two membranes that surround the mitochondrion. Apicomplexans are a phylum of intracellular parasites that cause major diseases in humans and animals, and are evolutionarily distant from model eukaryotes such as yeast. Apicomplexans harbour a mitochondrion that is essential for parasite survival, and is a validated drug target. Here, we demonstrate that the apicomplexan *Toxoplasma gondii* harbours homologues of proteins from all the major mitochondrial protein translocons present in yeast, suggesting these arose early in eukaryotic evolution. We demonstrate that a *T. gondii* homologue of Tom22 (*Tg*Tom22), a central component of the translocon of the outer mitochondrial membrane (TOM) complex, is essential for parasite survival, mitochondrial protein import, and assembly of the TOM complex. We also identify and characterize a *T. gondii* homologue of Tom7 (*Tg*Tom7) that is important for parasite survival and mitochondrial protein import. Contrary to the role of Tom7 in yeast, *Tg*Tom7 is important for TOM complex stability, suggesting the role of this protein has diverged during eukaryotic evolution. Together, our study identifies conserved and modified features of mitochondrial protein import in apicomplexan parasites.

Mitochondria arose through the endosymbiotic acquisition of an α-proteobacterium, likely in a single event that occurred early in eukaryotic evolution (1,2). Most known extant eukaryotes retain a mitochondrion or homologous organelle (3). Similar to their bacterial antecedents, most mitochondria retain a genome that encodes for some proteins. However, most proteins that function in the mitochondrion are nuclear encoded, and must post-translationally target across the two membranes that surround the mitochondrion. Proteins targeted to the mitochondrion contain either N-terminal presequences or internal targeting signals. These targeting signals interact with various protein translocons in the inner and outer membranes to ensure protein translocation across the mitochondrial membranes and into the appropriate compartment of the organelle.

Mitochondrial protein import is a core organellar function that was a critical early step in the evolution of mitochondria from α-proteobacteria (4). The last common ancestor of extant eukaryotes harboured a mitochondrion and also bore a functional mitochondrial protein import apparatus. However, it is becoming increasingly apparent that mitochondrial protein import machinery has diversified through the course of eukaryotic evolution.

Mitochondrial import has been most extensively studied in the yeast *Saccharomyces cerevisiae* (for a recent review see (5)). Translocation across the outer membrane is mediated by the *T*ranslocon of the *O*uter *M*itochondrial membrane (TOM^2)

complex. The TOM complex represents the entry point into the organelle for most mitochondrial proteins. In yeast, the TOM complex includes the β-barrel protein Tom40, which forms the central pore of the complex (6). The TOM complex also includes the receptor proteins Tom20 and Tom70, three small Tom proteins (Tom5, Tom6 and Tom7) that function in regulating TOM complex assembly and function, and Tom22, a single-pass transmembrane protein that has several functions. The cytosolic N-terminal region of yeast Tom22 functions as a receptor domain that interacts with proteins as they enter from the cytosol (7). The transmembrane domain is critical for assembling the TOM complex into a higher order structure (8). The intermembrane space–localized C-terminal domain of Tom22 interacts with presequence-containing proteins as they pass through the TOM complex, an interaction that is critical for translocation of these proteins to the translocase of the inner membrane (9).

The outer mitochondrial membrane contains several β-barrel proteins. The targeting of these proteins involves translocation into the intermembrane space through the TOM complex, and subsequent insertion into the outer membrane by an outer membrane insertase called the *S*orting and *A*ssembly *M*achinery (SAM) complex, the central component of which is known as Sam50 (10).

The presequence translocase, also known as the *T*ranslocon of the *I*nner *M*itochondrial membrane 23 (TIM23) complex, translocates presequence-containing proteins across the inner membrane. Tim23 forms the pore through this membrane, while Tim50 functions as a receptor for proteins as they translocate from the TOM complex (11,12). The presequence translocase can recruit a motor complex called the *P*resequence-translocase *A*sssociated *M*otor (PAM) to drive ATP-dependent translocation of proteins into the mitochondrial matrix. The central component of the PAM complex is a mitochondrial Hsp70 that associates with J-domain proteins such as Pam18 (13). Upon translocation into the matrix, the presequence is proteolytically cleaved by a mitochondrial processing peptidase (MPP) to yield the mature protein (14), which can then fold and carry out its function.

Many mitochondrial proteins lack N-terminal presequences, and instead harbour internal signals to direct them to the mitochondrion. Mitochondrial solute carrier proteins are inner membrane proteins that fall into this category. Mitochondrial carrier proteins enter the mitochondrion through the TOM complex, and then interact with small Tim proteins such as Tim9 and Tim10 in the intermembrane space. These function to deliver carrier proteins to the TIM22 complex, which inserts carrier proteins into the inner membrane. The core component of this insertase is the protein Tim22 (15).

While the mechanisms of mitochondrial import are well characterized in yeast and related organisms such as animals, this is less true of other eukaryotic lineages. The core components of the mitochondrial import machinery, including the TOM, TIM23, TIM22, PAM and SAM complexes, are present in plants (16). There are, however, several major differences between plants and yeast, most notably features of the TOM complex. Plants lack homologues of the receptor proteins Tom70 and Tom20, and have evolved alternative receptor proteins (17,18). Additionally, the plant Tom22 homologue is truncated at the N-terminus, and may not function as a presequence receptor (18,19).

Another phylum where the molecular mechanisms of mitochondrial import have been functionally examined is the trypanosomatids, a group of parasites that include *Trypanasoma brucei*, the causative agent of African sleeping sickness. The outer membrane translocon of trypanosomatids is termed the *A*rchaic *T*ranslocase of the *O*uter *M*itochondrial membrane (ATOM) complex, and appears different to the TOM complex in yeast. The central component of the ATOM complex is a β-barrel protein called Atom40 (20). There is debate as to whether Atom40 is homologous to Tom40 (21,22). Studies have identified other ATOM protein components, including Atom69, Atom46, Atom36, Atom14, Atom12 and Atom11 (23,24). These components lack clear homologues in yeast, although hidden Markov model analysis suggests that Atom14 is homologous to Tom22 (21). Trypanosomatid genomes harbour a single TIM translocase protein homologue, which is

essential for import of presequence-containing proteins (25,26).

Apicomplexans are a phylum of intracellular parasites. They include important human parasites such as *Plasmodium* species, the causative agents of malaria, and *Toxoplasma gondii*, a parasite that causes congenital disease in unborn children and encephalitis in immunocompromised people. Most apicomplexans harbour a mitochondrion, which is the target of major and emerging anti-apicomplexan drugs such as atovaquone, endochin-like quinolones and triazolopyrimidines (27-29). Studies of the mitochondrial protein import machinery of apicomplexans have been limited to comparative genomic approaches (30-32). These have identified putative homologues of the core components of mitochondrial import, including members of the TOM, TIM23, TIM22, PAM and SAM complexes.

The TOM complex of apicomplexans appears divergent from that found in yeast. Apicomplexan genomes lack identifiable homologues to TOM complex receptors such as Tom70 and Tom20. Like plants, the N-terminus of *Plasmodium* Tom22 appears truncated (19). Additionally, these comparative approaches have not identified Tom7 homologues in apicomplexan genomes, making apicomplexans one of the few lineages where a TOM complex is present that appears to lack Tom7 (19,21).

The last common ancestor of apicomplexans and yeast contained a mitochondrion and must have had a means of targeting nuclear-encoded proteins into this organelle. In this paper, we ask what features of this mitochondrial import apparatus have been conserved from the last common ancestor, and what new features have arisen? We use *T. gondii* as our model system to perform the first broad functional analysis of the mitochondrial protein import machinery in Apicomplexa. In particular we focus on the TOM complex, and assay the role of two TOM complex components in mitochondrial import and TOM complex biogenesis. These studies provide insights into conserved and novel functions of mitochondrial import machinery across their evolution, and provide a platform for future studies of mitochondrial import in an evolutionarily interesting, and medically important, group of organisms.

RESULTS

The identity and localization of putative mitochondrial import proteins in *T. gondii*

To identify candidate mitochondrial import proteins, we performed Basic Local Alignment Search Tool (BLAST) searches, querying the *T. gondii* genome with characterized mitochondrial import proteins from the yeast *S. cerevisiae*, the plant *Arabidopsis thaliana* and the trypanosomatid *T. brucei*. Matches were confirmed through reciprocal BLAST searches against the *T. gondii* genome. The results of these searches are summarised in Supplemental Table S1. We identified homologues of major subunits from each of the translocases and insertases involved in protein import into the mitochondrion. These include homologues of Tom40, Sam50, Tim23, Tim17, Tim50, Hsp70, Mge1, Tim44, Pam18, Tim22 and a host of small Tims. We also identified a *T. gondii* homologue of Oxa1, a protein that functions in the insertion of inner membrane proteins encoded on the mitochondrial genome ((33); Supplemental Table S1).

Some notable proteins lacked detectable homologs in *T. gondii*. This was particularly the case for the TOM complex, for which we were unable to identify candidates for receptor proteins (e.g. Tom70 and Tom20) or small Tom proteins (e.g. Tom5 and Tom7). Additionally, we were unable to identify components of the SAM and carrier insertase complexes beyond the central Sam50 and Tim22 subunits. We were also unable to identify a homologue of MIA40, a protein with a central role in the import of small Tim proteins into the intermembrane space (34).

To determine whether these candidate mitochondrial import proteins localized to the mitochondrion, we epitope-tagged select members of each protein complex. We first tagged *Tg*Tom40, the putative import pore in the outer membrane, and demonstrated co-localization with mitochondrially targeted RFP (Fig. 1A). Additionally, we generated polyclonal rabbit

antibodies against *Tg*Tom40. Immunofluorescence assays using this antibody supported the mitochondrial localization of *Tg*Tom40 (Fig. 1B). Analysis by western blotting revealed that *Tg*Tom40 is a protein with a mass of 48 kDa (Fig. 1C). Through co-localization with either Tom40 or mitochondrial RFP, and associated western blots, we demonstrated mitochondrial localization and protein expression for the following proteins: *Tg*Sam50 (Fig. 1D-E), consistent with the mitochondrial localization of this protein reported in a recent study (35); *Tg*Tim22 (Fig. 1F-G); *Tg*Tim23 (Fig. 1H-I); *Tg*Tim50 (Fig. 1J-K); and *Tg*MPPα (Fig. 1L-M). We were unable to generate a parasite strain that stably expressed epitope-tagged *Tg*Pam18. Instead, we transiently overexpressed c-myc-tagged *Tg*Pam18 in *T. gondii* parasites and performed an immunofluorescence assay. This revealed mitochondrial localization of *Tg*Pam18 (Fig. 1N). Taken together, these data indicate that *T. gondii* homologues of each of the major mitochondrial protein translocases and insertases localize to the mitochondrion (Fig. 1O).

Localization of the Tom22 homologue of *T. gondii*

Our bioinformatics survey (Supplemental Table S1) identified a *T. gondii* homologue of Tom22 that we called *Tg*Tom22. We performed an alignment of *Tg*Tom22 with Tom22 homologues from *Plasmodium falciparum*, yeast, humans and plants (Fig. 2A). This alignment revealed that the N-terminus of *Tg*Tom22 is truncated compared to yeast and human Tom22, as previously noted for Tom22 homologues in plants and *Plasmodium* (19). We identified two predicted transmembrane domains in *Tg*Tom22, one in an equivalent position to the transmembrane domain predicted for other Tom22 proteins, and a second at the very C-terminus of the protein (Fig. 2A). Sequence conservation amongst putative Tom22 homologues is generally poor, with only three identical residues found in all the proteins presented in the alignment, all three of which are found in the predicted transmembrane domain.

To localize *Tg*Tom22, and to facilitate subsequent functional analysis of this protein, we introduced an N-terminal haemagglutinin (HA) epitope tagged *Tg*Tom22 into the TATi strain of *T. gondii*. This exogenous version of *Tg*Tom22 was placed under the control of an anhydrotetracycline (ATc)-regulated promoter. We termed the resultant strain rTom22/eTom22, to indicate the presence of both regulatable and endogenous copies of *Tg*Tom22. We then knocked out the native Tom22 locus, verifying successful knockout by PCR analysis (Fig. 3A-B). The resultant strain was termed rTom22/Δ*tom22*, and expressed only the ATc-regulatable, HA-tagged *Tg*Tom22. Immunofluorescence analysis of this strain revealed that HA-Tom22 co-localizes with *Tg*Tom40, indicating that *Tg*Tom22 is a mitochondrial protein (Fig. 2B). Western blotting revealed that HA-Tom22 is 10 kDa in mass, close to the predicted mass of 12 kDa for the HA-tagged protein. To test whether *Tg*Tom22 is a transmembrane protein, we extracted *T. gondii* proteins in the rTom22/Δ*tom22* cell line with either the detergent Triton X-100 (TX-100) or sodium carbonate (Na_2CO_3) at pH 11.5. We determined that the HA-Tom22 protein localizes to the soluble fraction in Triton X-100 extraction, but to the membrane fraction upon Na_2CO_3 extraction (Fig. 2C). This is similar to the predicted integral membrane protein *Tg*Tom40 and distinct from the β-subunit of ATP synthase, a predicted soluble protein. We conclude that *Tg*Tom22 is a mitochondrial integral membrane protein.

Characterization of the TOM complex of *T. gondii*

As a first step to characterizing the TOM complex of *T. gondii* we performed blue-native polyacrylamide gel electrophoresis (BN-PAGE) on rTom22/Δ*tom22* strain *T. gondii* parasites, probing western blots with the *Tg*Tom40 antibody. When solubilised in either 0.5% or 1% digitonin, *Tg*Tom40 localizes to a protein complex of around 400 kDa (Fig. 4A). When solubilised in 1 % dodecylmaltoside (DDM) or 1% Triton X-100, *Tg*Tom40 localizes to a slightly smaller complex of around 325 kDa. The *Tg*Tom40 complex appeared insoluble in octyl β-D-glucopyranoside (OGP). We conclude that the *Tg*Tom40 protein is part of a ~400 kDa protein complex in the mitochondrion of *T. gondii*, which is similar in mass to characterized TOM complexes measured by BN-PAGE in yeast (36). We refer to this complex as the *T. gondii* TOM complex.

We have identified one other putative outer membrane protein involved in import, namely *Tg*Sam50, which is predicted to function in the outer membrane insertase complex. We hypothesised that *Tg*Tom22 localizes to the TOM complex, whereas *Tg*Sam50 localizes to a separate complex. To test this, we expressed a c-myc epitope tagged *Tg*Sam50 in the rTom22/Δ*tom22* cell line. We initially performed one-dimensional BN-PAGE and were unable to identify either HA-Tom22 or *Tg*Sam50-myc protein, likely because the epitope tags on these proteins were inaccessible to antibodies when in the complete complex[3]. We therefore performed two-dimensional BN-PAGE, separating protein complexes in the second dimension using SDS-PAGE. These studies revealed that *Tg*Tom40 is predominantly found in a 400 kDa complex that corresponds in mass to the TOM complex we observed in one-dimensional BN-PAGE (Fig. 4B). Lesser amounts of *Tg*Tom40 were observed in smaller complexes of around 300 kDa and 200 kDa (Fig. 4B). HA-Tom22 localizes exclusively in a 400 kDa complex that corresponds in mass to the 400 kDa complex containing *Tg*Tom40. *Tg*Sam50-myc localizes in complexes of 200 kDa and 350 kDa (Fig. 4B).

To further test the composition of the *T. gondii* TOM complex, we performed co-immunoprecipitation experiments on the *Tg*Sam50-cmyc/rTom22/Δ*tom22* cell line. We solubilised *T. gondii* proteins in 0.5% digitonin and immunoprecipitated *Tg*Tom40 and all interacting proteins using anti-*Tg*Tom40 antibodies. HA-Tom22, but not *Tg*Sam50, co-immuniprecipitated with *Tg*Tom40 antibodies (Fig. 4C).

Next, we performed pulldowns of HA-Tom22-interacting proteins using anti-HA antibodies. These studies revealed that a large fraction of *Tg*Tom40, but not *Tg*Sam50, associated with HA-Tom22 (Fig. 4C). Together, these results indicate that *Tg*Tom40 and *Tg*Tom22 form part of a core 400 kDa TOM complex that does not include *Tg*Sam50.

*Tg*Tom22 is essential for parasite growth

Having generated an ATc-regulatable *Tg*Tom22 cell line, we sought to determine whether *Tg*Tom22 was essential for parasite survival. We first measured knock down of HA-Tom22 by growing parasites for 0–2 days in ATc. This revealed that HA-Tom22 protein levels are much reduced 1 day after the addition of ATc, and undetectable after 2 days (Fig. 5A).

To determine whether *Tg*Tom22 is required for growth of *T. gondii* parasites, we introduced a tandem Tomato red fluorescent protein into the rTom22/Δ*tom22* cell line. This allows daily quantification of parasite growth as a function of well fluorescence in a 96-well plate (37,38). rTom22/Δ*tom22* parasites cultured in the presence of ATc showed no detectable growth across the 8-day experiment (Fig. 5B). These data indicate that *Tg*Tom22 is critical for parasite growth. To determine whether the observed defect in growth in the presence of ATc is dependent on *Tg*Tom22, we complemented the rTom22/Δ*tom22* cell line with constitutively-expressed *Tg*Tom22, producing the strain we termed rTom22/Δ*tom22*/Tom22wt. Parasite growth in this strain was equivalent with or without ATc (Fig. 5C), consistent with the observed growth effect in mutant parasites resulting solely from loss of *Tg*Tom22.

*Tg*Tom22 is essential for mitochondrial protein import

We next wanted to determine the function(s) of *Tg*Tom22. We hypothesised that *Tg*Tom22 plays a role in mitochondrial protein import. Proteins targeted to the matrix of mitochondria harbour an N-terminal presequence that is removed upon entry into the matrix. Presequence cleavage, therefore, serves as a robust measure for mitochondrial protein import. To monitor this, we fused the presequence leader of the mitochondrial protein *Tg*Hsp60 ($Hsp60_L$) to a c-myc tagged mouse DHFR (mDHFR) reporter protein (mDHFR has been used extensively in studies of mitochondrial import in other systems), and introduced this $Hsp60_L$-mDHFR-cmyc protein construct into rTom22/Δ*tom22* parasites. We grew parasites for 0 to 3 days on ATc and measured the abundance of a range of proteins by western blot. As shown previously, HA-Tom22 was

undetectable after 2 days on ATc (Fig. 6A). In the presence of HA-Tom22, we observe a single $Hsp60_L$-mDHFR-cmyc band that corresponds in mass to the mature (processed) form of this protein, where the presequence has been removed (Fig. 6A). Upon loss of HA-Tom22, we see an accumulation of the precursor form of $Hsp60_L$-mDHFR-cmyc, as well as the precursor form of the native *Tg*Hsp60 protein (Fig. 6A). Notably, Tom40 levels remain unchanged with the loss of HA-Tom22.

As a more sensitive measure of mitochondrial protein import we performed a radioactive-labelling experiment. We incubated rTom22/Δ*tom22* parasites expressing $Hsp60_L$-mDHFR-cmyc for 10, 30 and 60 minutes in medium containing [^{35}S]-labelled methionine and cysteine. We then performed immunoprecipitations to purify $Hsp60_L$-mDHFR-cmyc protein and separated proteins by SDS-PAGE. In the absence of ATc, we observed two protein bands, corresponding in mass to the precursor and mature forms of $Hsp60_L$-mDHFR-cmyc (Fig. 6B). Only a small amount of mature $Hsp60_L$-mDHFR-cmyc was present at the 10 minute time point in the absence of ATc, but this increased upon longer incubation in the radioactive medium, consistent with protein synthesis followed by precursor processing upon mitochondrial import. In contrast, we observed only the precursor form of $Hsp60_L$-mDHFR-cmyc in parasites grown for 2 days on ATc, indicative of an absence of mitochondrial protein import in these parasites. We conclude that *Tg*Tom22 is critical for mitochondrial protein import.

*Tg*Tom22 is critical for TOM complex assembly

We next sought to determine the functional roles of *Tg*Tom22. We first asked whether *Tg*Tom22 has a role in TOM complex assembly. We performed BN-PAGE on proteins extracted from rTom22/Δ*tom22* parasites grown for 0 to 3 days on ATc. We observed a marked decrease in the 400 kDa TOM complex after one day on ATc, and complete loss of this complex after 2 days (Fig. 6C), concomitant with loss of the HA-Tom22 protein.

The apparent absence of the TOM complex in this experiment was puzzling, since *Tg*Tom40 protein levels remain unchanged upon loss of HA-Tom22 (Fig. 6A). We wondered whether loss of HA-Tom22 upon the addition of ATc resulted in a complex that masked *Tg*Tom40 protein to antibodies in this one-dimensional BN-PAGE approach. We performed two-dimensional BN-PAGE on rTom22/Δ*tom22* parasites grown in the absence of ATc or in the presence of ATc for 2 days. In the absence of ATc, most Tom40 was present in the 400 kDa TOM complex, whereas some was also present in ~200 kDa and ~300 kDa complexes (Fig. 6D), as observed previously (Fig. 4B). Upon loss of HA-Tom22, we could detect Tom40, but this was exclusively in the 200 kDa and 300 kDa protein complexes.

To further test the role of *Tg*Tom22 in TOM complex assembly, we fused an FKBP-based destabilisation domain (DD; (39)) to the N-terminus of wild-type *Tg*Tom22 and introduced this into rTom22/Δ*tom22* parasites to derive the parasite strain rTom22/Δ*tom22*/DD-Tom22wt. The stability of DD-tagged proteins can be controlled through the addition of the small molecule Shld1, allowing for rapid control of protein levels (39). We monitored the growth of both rTom22/Δ*tom22* and rTom22/Δ*tom22*/DD-Tom22wt parasites using the previously described fluorescence growth assay, incubating parasites either in the absence of ATc and Shld1, in the presence of ATc and absence of Shld1, or in the presence of both ATc and Shld1 (to turn off expression of regulatable HA-Tom22 and to stabilise DD-Tom22wt). Growth of rTom22/Δ*tom22* parasites was negligible in the presence of ATc, regardless of the presence of Shld1 (Fig. 6E). In the rTom22/Δ*tom22*/DD-Tom22wt parasite strain, however, parasite growth in the presence of ATc was restored to near wild-type levels upon the addition of Shld1 (Fig. 6F). This indicates that DD-Tom22wt can complement the rTom22/D*tom22* mutant.

We grew rTom22/Δ*tom22*/DD-Tom22wt parasites for 0 or 48 hours in ATc. For the parasites grown for 48 hours in ATc, we added Shld1 0, 3, 6, 18 or 48 hours before harvesting. We then performed BN-PAGE on proteins extracted from these cell lines. In the absence of ATc, *Tg*Tom40 is found in

the ~400 kDa TOM complex, whereas the addition of ATc disrupts the 400 kDa complex in the absence of Shld1 (0 hours; Fig. 6G). Three hours after the addition of Shld1, we see re-formation of the 400 kDa TOM complex, and the abundance of the TOM complex increases with increased time on Shld1 (Fig. 6G). Three and 6 hours after the addition of Shld1, we observe some *Tg*Tom40 in smaller protein complexes of ~150 kDa and ~300 kDa, which may represent intermediates in TOM complex assembly. We conclude that *Tg*Tom22 has a critical, and likely direct, role in TOM complex assembly.

Apicomplexan parasites have a Tom7 homologue that is important for TOM complex assembly and parasite growth

T. gondii harbours a TOM complex of around 400 kDa that contains *Tg*Tom40 and *Tg*Tom22. We reasoned that other proteins must be part of this complex as well. Previous bioinformatics approaches have been unable to identify homologues of small TOM complex proteins such as Tom7 in apicomplexans, even though these are present in the genomes of many other eukaryotes (19,21). Given the limited primary sequence conservation, we reasoned that homology searches might be insufficient to identify Tom7 homologues in these parasites. From an alignment of Tom7s from multiple organisms, we noted that the conserved feature of all of these is a $G(X)_2P(X)_5G$ motif in the single transmembrane domain. We searched the genome of the apicomplexan parasite *P. falciparum* for predicted proteins that harbour this motif. We then screened these candidates further for proteins of less than 15 kDa that harboured a single transmembrane domain. This produced one candidate, a hypothetical protein annotated as PF3D7_0823700. Using this as a query sequence, we identified a homologous protein encoded on the *T. gondii* genome (TGME49_210255) and termed this *Tg*Tom7. We performed 5' rapid amplification of cDNA ends (5'-RACE) to identify the open reading frame and establish its sequence.

We constructed an alignment of the putative *Tg*Tom7 protein with Tom7 homologues in other organisms, revealing the presence of the $G(X)_2P(X)_5G$ in the transmembrane domain, but little further conservation (Fig. 7A). The *Tg*Tom7 open reading frame contains two potential start codons. Alignments of *Tg*Tom7 sequence with the homologous protein in *Neospora caninum*, a close relative of *T. gondii*, revealed no conservation upstream of the second start codon (Fig. 7A). Furthermore, subsequent analysis revealed that the longer form of *Tg*Tom7 exhibits similar localization and mutant phenotypes to the short form, suggesting that the region upstream of the second start codon is dispensable for function[3]. Together, these data suggests that the second codon may represent the true start codon in this gene.

To localize *Tg*Tom7, we fused a region encoding a 3xHA tag to the 5' end of the open reading frame to enable detection of the resultant protein (which we termed HA_3-Tom7). To facilitate subsequent functional analysis, we also replaced the native promoter of this gene with an ATc-regulated promoter in the TATi/Δ*ku80* parasite strain (41) to generate the parasite strain we termed TATi/Δ*ku80*/rTom7. We confirmed successful integration of the 5'-HA tag and ATc-regulated promoter through PCR analysis (Fig. 3C-D). We performed an immunofluorescence assay, which demonstrated co-localization of HA_3-Tom7 with *Tg*Tom40 (Fig. 7B), indicating that *Tg*Tom7 is a mitochondrial protein. Western blot analysis indicated that HA_3-Tom7 is 11 kDa in mass (Fig. 7C), correlating to the predicted molecular mass of 11 kDa for HA_3-Tom7.

Two-dimensional BN-PAGE analysis revealed that *Tg*Tom7 exists in a protein complex of around 400 kDa, corresponding in mass to the TOM complex (Fig. 7D). Curiously, and in contrast to our previous analyses performed on the rTom22/Δ*tom22* strain of parasites, we did not observe the ~300 kDa and ~200 kDa protein complexes in the *Tg*Tom40 western blot. This may suggest that the rTom22/Δ*tom22* mutant has some defects in TOM complex assembly even in the absence of ATc, possibly due to the presence of the N-terminal HA tag, or resulting from slight modification of native expression levels in using the ATc-regulated promoter.

We performed a co-immunoprecipitation with antibodies against *Tg*Tom40. Most of the HA_3-Tom7 protein appeared in the bound fraction (Fig. 7E), indicating that HA_3-Tom7 is part of a complex with *Tg*Tom40. We attempted the reciprocal experiment of co-immunoprecipitating with anti-HA-coupled beads. We were unable to purify either HA_3-Tom7 or *Tg*Tom40[3], suggesting that the HA-tag on *Tg*Tom7 may be hidden from antibodies within the complex.

We next asked whether *Tg*Tom7 was important for parasite growth. First, we determined whether the addition of ATc resulted in knockdown of the HA_3-Tom7 protein. We cultured parasites in ATc for 0–3 days and measured protein abundance. HA_3-Tom7 protein was undetectable after 2 days growth on ATc (Fig. 8A). To test whether *Tg*Tom7 is important for parasite growth, we introduced a tandem Tomato red fluorescent protein into the rTom22/Δ*tom22* cell line. We performed fluorescence growth assays on Tomato-expressing parental (TATiΔ*ku80*) and TATi/Δ*ku80*/rTom7 parasites. These revealed that TATi/Δ*ku80*/rTom7 strain parasites alone exhibited growth impairment in the presence of ATc (Fig. 8B-C).

To ascertain whether this growth phenotype resulted solely from downregulation of *Tg*Tom7 expression, we complemented the TATi/Δ*ku80*/rTom7 strain with *Tg*Tom7 expressed from a constitutive promoter to produce a cell line termed TATi/Δ*ku80*/rTom7/Tom7wt. We then introduced a tandem Tomato red fluorescent protein and performed fluorescent growth assays. This revealed that this complemented strain was fully restored in growth (Fig. 8D), suggesting that the growth defect we observed results entirely from the decrease in *Tg*Tom7 expression.

We next wanted to determine whether *Tg*Tom7 has a role in mitochondrial protein import. Attempts to generate a TATi/Δ*ku80*/rTom7 strain expressing the mitochondrial $Hsp60_L$-mDHFR-cmyc construct were unsuccessful. Instead, we performed a western blot on TATi/Δ*ku80*/rTom7 parasites grown for 0–3 in ATc, and probed with antibodies against mitochondrial *Tg*Hsp60. When Tom7 is present (day 0), we observe a single *Tg*Hsp60 protein species that corresponds to the mature, mitochondrially localized *Tg*Hsp60 protein (Fig. 8A). Two days after the addition of ATc, and concomitant with *Tg*Tom7 knockdown, we observe the appearance of a higher molecular mass species, corresponding to presequence-containing *Tg*Hsp60. This band increases in abundance after 3 days on ATc (Fig. 8A). Notably, the abundance of *Tg*Tom40 remains unchanged upon the addition of ATc. These data are consistent with a role for *Tg*Tom7 in mitochondrial protein import that does not depend on regulating the stability or turnover of *Tg*Tom40.

Given the role of *Tg*Tom22 in TOM complex assembly, we wanted to determine whether *Tg*Tom7 was also important for this process. We performed BN-PAGE to measure TOM complex assembly upon HA_3-Tom7 knockdown. These studies revealed loss of the TOM complex concomitant with HA_3-Tom7 knockdown (Fig. 8E). We performed two-dimensional BN-PAGE on TATi/Δ*ku80*/rTom7 parasites grown in the absence of ATc or in the presence of ATc for 2 days. In the absence of ATc, Tom40 was present in the ~400 kDa TOM complex. Upon HA_3-Tom7, knockdown, Tom40 was present in smaller complexes of approximately 240 kDa, 150 kDa and 50 kDa. These observations are consistent with a role for *Tg*Tom7 in TOM complex formation and/or assembly.

DISCUSSION

The means to import proteins into mitochondria must have arisen early in mitochondrial, and therefore eukaryotic, evolution (42). Less clear are the origins of the proteins and protein complexes involved in this process, and how these have changed over time. Recent studies of mitochondrial import in plants and trypanosomes have revealed that canonical yeast features such as an outer membrane TOM complex and separate inner membrane TIM23 and TIM22 complexes are either extensively modified or lacking from these organisms (17,20,21,23,26). We demonstrate here that *T. gondii* harbours mitochondrially localized candidate proteins from all the major mitochondrial translocons and insertases (Fig. 1O; Supplemental Table S1). This implies that the last

common ancestor of apicomplexans and yeast had homologues of these mitochondrial import components, and that these likely functioned in the mitochondrion. The fact that homologues of these complexes are found in other eukaryotes, such as plants and the amoeba *Dictyostelium* (43), suggests that the common ancestor of all these major eukaryotic lineages harboured homologues of these proteins.

Comparative genomics implies but cannot truly assess conservation of protein function. We therefore set about characterizing select aspects of mitochondrial protein import in *T. gondii*, with a particular view to understanding whether the function of candidate translocon components has changed across evolution. We focused our attention on the putative *T. gondii* TOM complex, which our comparative genomic approach indicated had interesting differences to the TOM complex of yeast.

We demonstrate that the TOM complex of *T. gondii* is approximately 400 kDa in mass (Fig. 4), corresponding to the mass of the core TOM complex in yeast, but considerably larger than the ~230 kDa complex found in plants (44,45). The *T. gondii* TOM complex contains *Tg*Tom40, *Tg*Tom22 and *Tg*Tom7, and excludes *Tg*Sam50. Instead, *Tg*Sam50 exists predominantly in a protein complex of ~200 kDa, similar in mass to the SAM complex of yeast (46,47), although a larger complex of ~350 kDa is also apparent.

We were unable to identify homologs to known TOM receptor proteins in apicomplexans. One striking feature of TOM complex receptors is that no two major eukaryotic lineages yet examined have identifiable homologous receptor proteins. Tom20 and Tom70 are unique to opisthokonts, plant Tom20 and mtToc64 are unique to plants, ATOM69 and ATOM46 are unique to trypanosomatids, and no homologues of these proteins are apparent in apicomplexans. This suggests that TOM receptor proteins were either absent from the last common ancestor of these eukaryotes, or that novel receptors have replaced the original ones. One theory of mitochondrial evolution posits that the evolution of receptor proteins on the TOM complex will have created a powerful selective advantage (42). An intriguing possibility is that the evolution of TOM complex receptors occurred multiple times in separate lineages, and that this contributed to the radiation, and subsequent success, of the extant eukaryotic lineages. Identifying and characterizing the TOM complex receptors in apicomplexans is now a major priority in this area.

We demonstrate that loss of *Tg*Tom22 leads to defects in maturation of mitochondrial matrix proteins, consistent with a role for *Tg*Tom22 in mitochondrial protein import. Studies from yeast have identified a key role for Tom22 in TOM complex assembly (8). Our data suggest *Tg*Tom22 has a direct role in TOM complex assembly, mirroring the role of Tom22 in yeast. In yeast, loss of Tom22 results in disassembly of the TOM complex to form a ~100 kDa complex. In *T. gondii*, *Tg*Tom22 knockdown leads to the formation of two major protein complexes of 200 kDa and 300 kDa (Fig. 6D). It is unclear whether these are simply disassembled TOM complexes, or precursors of the TOM complex, although it is interesting to note that SAM50 forms complexes of ~200 kDa (Fig. 4B), suggesting the smaller of the complexes could be a SAM-TOM complex intermediate. Also unclear is whether these depleted *Tg*Tom40-containing complexes can function in import. Regardless, the conserved role of Tom22 in TOM complex assembly between yeast and apicomplexans suggests that one role of Tom22 in the last common ancestor of these lineages was assembly of the TOM complex. This points to an ancient and conserved role for Tom22 in TOM complex assembly.

In yeast, Tom7 is a non-essential protein that negatively regulates TOM complex assembly (48,49). Loss of Tom7 in yeast, therefore, promotes TOM complex assembly. Previously, apicomplexans were thought to be one of only a few TOM complex-containing eukaryotic lineages that lacked a Tom7 homologue (19). We revisited this and were able to identify a candidate Tom7 homologue in both *T. gondii* and *P. falciparum*. We could demonstrate that *Tg*Tom7 was indeed a component of the core TOM complex in these parasites and important for mitochondrial protein import.

In contrast to yeast, loss of *Tg*Tom7 leads to a growth defect in *T. gondii* parasites and impairment of TOM complex assembly. We observe TOM complex dissociation concomitantly with *Tg*Tom7 knockdown, suggesting the two processes are directly linked. Nevertheless, we were unable to generate a tightly regulated DD-tagged *Tg*Tom7 cell line, which precluded a more robust test of this hypothesis. Notably, although knockdown of both *Tg*Tom7 and *Tg*Tom22 result in dissociation of the TOM complex, loss of *Tg*Tom22 leads to a considerably stronger growth defect (cf. Fig. 5B and Fig. 8C), and a qualitatively more severe defect in mitochondrial protein import (cf. Fig. 6A and Fig. 8A). This suggests that protein import is not entirely ablated upon TOM complex disassembly. It also suggests that, in addition to its role in TOM complex assembly, *Tg*Tom22 has other roles in mitochondrial protein import. The C-terminal, intermembrane space domain of Tom22 in other organisms is critical for translocating proteins from the TOM complex to the presequence translocase (9), and it is conceivable that *Tg*Tom22 has a role in this process.

Apicomplexan Tom7 is the first non-opisthokont Tom7 that has been functionally characterized. The contrasting role of Tom7 between apicomplexans and opisthokonts suggests that, even though it is conserved as part of the "core" TOM complex, the functions of Tom7 have diverged substantially during eukaryotic evolution. This is in contrast to our findings with Tom22, where the role of Tom22 in TOM complex assembly appears conserved. From our functional analyses, we can conclude that the TOM complex of apicomplexan parasites contains both conserved and unique features when compared to the TOM complex of yeast.

EXPERIMENTAL PROCEDURES

Parasite culture and growth assays. Parasites were grown in human foreskin fibroblasts using Dulbecco's modified Eagle's medium supplemented with 1% fetal calf serum and antibiotics. Strains used included RH, TATi, Δ*ku80* and TATi/Δ*ku80* (41,50,51). All parasite strains described in this manuscript were cloned by limiting dilution. Where required, we added anhydrotetracycline (ATc) at a final concentration of 0.5 µg/ml and Shield-1 (Shld1) at a final concentration of 0.75 µM. Fluorescence growth assays were performed in optical bottom 96-well plates as described previously (37,38), and read using a FluoStar Optima fluorescence plate reader (BMG Labtech).

Plasmid construction. To determine the localization of the candidate mitochondrial import-related proteins, we introduced epitope tags at the 3' end of either the endogenous locus of the genes encoding these proteins, or of the open reading frame of candidate genes expressed from constitutive promoters. To localize *Tg*Tom40, we amplified the 3' region with primers 1 and 2 (Table 1), inserted this into the vector pHA_3.LIC.DHFR (a kind gift from Michael White, U. South Florida) by ligation independent cloning (LIC) as described previously (50), before linearization with *Eco*RV, transfection into Δ*ku80* strain parasites, and selection on pyrimethamine as described (52). To localize *Tg*Sam50, we amplified the open reading frame with primers 3 and 4, digested the resulting product with *Bgl*II and *Avr*II, ligated into the vector $pBTM_3$ (53), transfected into parasites, and selected on phleomycin as described (54). To localize *Tg*Tim22, we amplified the 3' region with primers 5 and 6, digested the resulting product with *Bgl*II and *Avr*II and ligated into pHH vector, a modified version of the pgCM3 vector described previously (55), that has a selectable marker for mycophenolic acid selection. The vector was linearized with *Afl*II, transfected into parasites, and selected on mycophenolic acid as described (52). To localize *Tg*Tim23, we amplified the 3' region with primers 7 and 8, digested the resulting product with *Bgl*II and *Avr*II and ligated into the pBH vector, a modified version of the pHH vector that contains a phleomycin-resistance marker. This vector was linearized with *Nco*I, transfected into parasites, and selected on phleomycin. To localize *Tg*Tim50, we amplified the 3' region with primers 9 and 10, inserted the product into the vector pTy.LIC.DHFR, a modified version of pHA_3.LIC.DHFR where the HA-tag has been replaced by a 1xTy1 tag, through LIC. The resulting vector was digested with *Nsi*I, transfected into parasites and selected on

pyrimethamine. To localize *Tg*Pam18, we amplified the open reading frame with primers 11 and 12, digested the resulting product with *Bgl*II and *Avr*II, and ligated into the vector pBTM$_3$. We transfected the resulting vector into parasites and observed transient expression after one day. To localize *Tg*MPPα, we amplified the 3' region with primers 13 and 14, inserted this into pHA$_3$.LIC.DHFR by LIC, linearized with *Nco*I, transfected into parasites, and selected on pyrimethamine.

To generate an ATc-regulated knockdown strain of *Tg*Tom22, we amplified the *Tg*Tom22 open reading frame with primers 15 and 16, digested the resulting product with *Xma*I and *Aat*II and ligated into the equivalent sites of the pDt7s4H vector (56). This vector was transfected into TATi strain parasites and selected on pyrimethamine. To knockout the native *Tg*Tom22 gene, we amplified a region upstream of the *Tg*Tom22 start codon with primers 17 and 18, digested the resulting product with *Spe*I and *Bgl*II, and ligated into the equivalent sites on the vector pTCY (38). We then amplified a region downstream of the *Tg*Tom22 stop codon using primers 19 and 20, digested the resulting product with *Sal*I and *Apa*I, and ligated into equivalent sites of the pTCY vector containing the *Tg*Tom22 5' flank. We transfected this into parasites expressing the ATc-regulated copy of *Tg*Tom22, selected parasites on chloramphenicol as described (52), and subjected parasites to negative YFP selection as described (57). We screened clones for *Tg*Tom22 knockout using primers 21 and 22.

To generate a strain expressing the mitochondrial targeting sequence of *Tg*Hsp60 fused to c-myc tagged mouse DHFR, we digested the *Tg*Hsp60 leader sequence from the vector Hsp60-RFP in pBTR (58) with *Bgl*II and *Avr*II, ligated this into the equivalent sites of the vector mDHFR in pBTM$_3$ (53), transfected into the *Tg*Tom22 knockdown cell line, and selected on phleomycin.

To generate a parasite strain expressing *Tg*Tom22 fused to an N-terminal DD tag, we amplified the open reading frame of *Tg*Tom22 with the primers 23 and 24, digested with *Xma*I and *Aat*II, and ligated this into the equivalent sites of the vector pCTDDnM, a modified version of the vector pCTDDnH (58), which contains a c-myc tag in place of an HA tag. We then replaced the chloramphenicol-resistance marker in this vector with a phleomycin-resistance marker (to generate the vector pBTDDnM-*Tg*Tom22), transfected into *Tg*Tom22 knockdown parasites and selected on phleomycin.

To determine the correct 5' region of the *Tg*Tom7 cDNA, we performed 5' RACE using the SMARTer RACE cDNA amplification kit (Clontech) according to the manufacturer's instructions. We used primer 25 for the first reaction and primer 26 for the nested reaction.

To determine the localization and function of *Tg*Tom7, we replaced the native promoter of *Tg*Tom7 with an ATc-regulated promoter, introducing an N-terminal 3xHA tag onto *Tg*Tom7 in the process. We amplified a 3' flank of *Tg*Tom7 with primers 27 and 28, digested the product with *Xma*I and *Not*I, and ligated into the equivalent sites of the vector pPR2-HA$_3$ (55). We next amplified the 5' flank of the *Tg*Tom7 gene with primers 29 and 30, digested the product with *Apa*I and *Asc*I, and ligated into the equivalent sites of the pPR2-HA$_3$ vector harbouring the *Tg*Tom7 3' flank. We linearised this vector with *Not*I, transfected into TATi/Δ*ku80* strain parasites (41), and selected on pyrimethamine. Clones were screened for successful promoter replacement by PCR, using primers 31 and 32, which only gives band if the native locus is present, and primers 32 and 33, which only give a band if the 5' region of *Tg*Tom7 is replaced by the regulated promoter.

To complement the *Tg*Tom7 knockdown mutant, we amplified the entire open reading frame of *Tg*Tom7 with primers 34 and 35 using *T. gondii* cDNA as template. We digested the product with *Nco*I and *Mfe*I, ligated this into the equivalent sites of the pBTDDnTy vector, a modified version of the pBTDDnM vector that has a 5'-Ty1 epitope tag instead of a c-myc tag. We digested the resulting vector with *Avr*II and *Not*I, which excises the Ty1-*Tg*Tom7 open reading frame, and ligated this into equivalent sites of pUgCTH$_3$ (Rajendran et al, in preparation), which places Ty1-tagged *Tg*Tom7 downstream of the constitutive α-tubulin promoter. We linearised this vector with *Aat*II,

transfected into the *Tg*Tom7 knockdown cell line, and selected parasites on chloramphenicol.

*Anti-*Tg*Tom40 antibody generation.* To generate an antibody against *Tg*Tom40, we PCR amplified a region of the *Tg*Tom40 open reading frame (encoding residues 2-173 of the *Tg*Tom40 protein) with primers 36 and 37, and integrated the product into the vector pAVA0421 by LIC (59). The plasmid was transformed into BL21 strain *Escherichia coli*, and *Tg*Tom40 expression induced through the addition of IPTG. His-tagged *Tg*Tom40 was purified using Ni-NTA agarose resin (Qiagen) according to the manufacturer's instructions, and purified protein was used to immunise rabbits (IVMS Vet Services, Adelaide, Australia).

BN-PAGE. For preparation of proteins for blue native-polyacrylamide gel electrophoresis (BN-PAGE), parasites were filtered through a 3 µm filter and pelleted by centrifugation at 1500 g, 10 min, 4°C. Parasites were washed once in ice-cold phosphate-buffered saline (PBS), then solubilised to a final concentration of 2.5×10^5 parasites/µl in NativePAGE buffer (Life Technologies), supplemented with EDTA-free Complete protease inhibitor cocktail (Roche Applied Sciences), 2 mM EDTA, and an appropriate detergent. Samples were incubated for 30 min at 4°C, then centrifuged at 20,000 g for 30 min at 4°C to remove insoluble material. Samples were separated on a 4–16% NativePAGE Bis-Tris gel (Life Technologies) according to the manufacturer's instructions, then transferred to PVDF membrane, or subjected to a second dimension SDS-PAGE gel (Life Technologies) according to the manufacturer's instructions, before transfer to nitrocellulose membrane and subsequent western blotting.

Sodium carbonate extractions, immunoprecipitations and [^{35}S]-radiolabeling. Sodium carbonate extractions and immunoprecipitations were performed as described previously (38). Antibodies used for immunoprecipitations were rat anti-HA conjugated to agarose beads (Roche Applied Sciences), mouse anti-c-myc conjugated to agarose beads (Thermo Scientific), and anti-*Tg*Tom40 antibodies conjugated to Protein A Sepharose CL-4B beads (Pierce). Co-immunoprecipitations were performed on parasite extracts solubilised in 0.5% digitonin in a buffer consisting of 50 mM Tris-HCl, pH 8.0, 150 mM NaCl, 2 mM EDTA and Complete protease inhibitors. [^{35}S]-radiolabeling was performed as described previously (38), except that parasites were incubated in Expre^{35}S^{35}S protein labelling mix (Perkin Elmer) for 10-60 min before harvesting.

Western blotting and immunofluorescence assays. Western blotting and immunofluorescence assays were performed as described previously (38). Samples were probed with the following antibodies: rat anti-HA (1:100 to 1:500, Roche Applied Science), mouse anti-c-myc (1:100 to 1:500, Thermo Scientific), mouse anti-Ty1 (1:200 to 1:1000, (60)), mouse anti-GRA8 (1:100,000, a kind gift from Gary Ward, U. Vermont, (61), rabbit anti-*Tg*Tom40 (1:2000, this study), rabbit anti-*E. coli* GroEL (1:1000; which we have previously shown also binds the mitochondrial Hsp60 of apicomplexan parasites; (62)), rabbit anti-ATP synthase β-subunit (1:3000, Agrisera), AlexaFluor 488-conjugated goat anti-rat IgG (1:200, Life Technologies), AlexaFluor 488-conjugated goat anti-mouse IgG (1:200 to 1:500, Life Technologies), AlexaFluor 546-conjugated goat anti-rabbit IgG (1:500, Life Technologies), horse radish peroxidase (HRP)-conjugated goat anti-rabbit IgG (1:5000 to 1:10,000, Thermo Scientific), HRP-conjugated goat anti-mouse IgG (1:5,000 to 1:10,000, Thermo Scientific), HRP-conjugated goat anti-rat IgG (1:5,000; Thermo Scientific), TrueBlot HRP-conjugated anti-mouse IgG (1:1000, Rockland Immunochemicals) and TrueBlot HRP-conjugated anti-rabbit IgG (1:1000, Rockland Immunochemicals). Fluorescence images were acquired on a Leica TCS SP2 inverted laser scanning confocal microscope, or a DeltaVision Elite system (GE Healthcare) using an inverted Olympus IX71 microscope. DeltaVision images were deconvolved using SoftWoRx Suite 2.0 software. All images were adjusted for contrast and brightness.

ACKNOWLEDGEMENTS

We thank Ming Kalanon for helpful discussions, Gary Ward and Michael White for sharing reagents, and Harpreet Vohra and Julie Nelson for assistance with flow cytometry. This work was supported by a Discovery Grant from the Australian Research Council (ARC) to GvD (DP110103144), a National Health and Medical Research Program Grant to GIM, and a grant from the National Institutes of Health to BS (RO1AI 64671). GvD is an ARC QEII fellow and BS is a Georgia Research Alliance Distinguished Investigator.

CONFLICTS OF INTEREST

The authors declare that they have no conflicts of interest with the contents of this article.

AUTHOR CONTRIBUTIONS

GvD, BS and GIM conceived the study. GvD and LMY designed and performed the experiments. GvD, LMY, BS and GIM analysed the data. GvD wrote the manuscript with contributions from all the authors.

FOOTNOTES

[1] To whom correspondence may be addressed. E-mail: giel.vandooren@anu.edu.au.

[2] The abbreviations used are: TOM, Translocon of the Outer Mitochondrial membrane; SAM, Sorting and Assembly Machinery; TIM, Translocon of the Inner Mitochondrial membrane; PAM, Presequence-translocase Associated Motor; MPP, Mitochondrial Processing Peptidase; ATOM, Archaic Translocase of the Outer Mitochondrial membrane; ATc, anhydrotetracycline; Shld1, Shield-1; LIC, Ligation Independent Cloning; BN-PAGE, Blue Native-Polyacrylamide Gel Electrophoresis; BLAST, Basic Local Alignment Search Tool; TX-100, Triton X-100; DDM, dodecylmaltoside; OGP, octyl β-D-glucopyranoside.

[3] Unpublished observation.

REFERENCES

1. Embley, T. M., and Martin, W. (2006) Eukaryotic evolution, changes and challenges. *Nature* **440**, 623-630
2. Sagan, L. (1967) On the origin of mitosing cells. *J Theor Biol* **14**, 255-274
3. van der Giezen, M., and Tovar, J. (2005) Degenerate mitochondria. *EMBO Rep* **6**, 525-530
4. Dolezal, P., Likic, V., Tachezy, J., and Lithgow, T. (2006) Evolution of the molecular machines for protein import into mitochondria. *Science* **313**, 314-318
5. Dudek, J., Rehling, P., and van der Laan, M. (2013) Mitochondrial protein import: Common principles and physiological networks. *Biochim Biophys Acta* **1833**, 274-285
6. Hill, K., Model, K., Ryan, M. T., Dietmeier, K., Martin, F., Wagner, R., and Pfanner, N. (1998) Tom40 forms the hydrophilic channel of the mitochondrial import pore for preproteins. *Nature* **395**, 516-521
7. Brix, J., Dietmeier, K., and Pfanner, N. (1997) Differential recognition of preproteins by the purified cytosolic domains of the mitochondrial import receptors Tom20, Tom22, and Tom70. *J Biol Chem* **272**, 20730-20735
8. van Wilpe, S., Ryan, M. T., Hill, K., Maarse, A. C., Meisinger, C., Brix, J., Dekker, P. J., Moczko, M., Wagner, R., Meijer, M., Guiard, B., Honlinger, A., and Pfanner, N. (1999) Tom22 is a multifunctional organizer of the mitochondrial preprotein translocase. *Nature* **401**, 485-489
9. Moczko, M., Bomer, U., Kubrich, M., Zufall, N., Honlinger, A., and Pfanner, N. (1997) The intermembrane space domain of mitochondrial Tom22 functions as a trans binding site for preproteins with N-terminal targeting sequences. *Mol Cell Biol* **17**, 6574-6584
10. Gentle, I., Gabriel, K., Beech, P., Waller, R., and Lithgow, T. (2004) The Omp85 family of proteins is essential for outer membrane biogenesis in mitochondria and bacteria. *J Cell Biol* **164**, 19-24
11. Geissler, A., Chacinska, A., Truscott, K. N., Wiedemann, N., Brandner, K., Sickmann, A., Meyer, H. E., Meisinger, C., Pfanner, N., and Rehling, P. (2002) The mitochondrial presequence translocase: an essential role of Tim50 in directing preproteins to the import channel. *Cell* **111**, 507-518
12. Truscott, K. N., Kovermann, P., Geissler, A., Merlin, A., Meijer, M., Driessen, A. J., Rassow, J., Pfanner, N., and Wagner, R. (2001) A presequence- and voltage-sensitive channel of the mitochondrial preprotein translocase formed by Tim23. *Nat Struct Biol* **8**, 1074-1082
13. Truscott, K. N., Voos, W., Frazier, A. E., Lind, M., Li, Y., Geissler, A., Dudek, J., Muller, H., Sickmann, A., Meyer, H. E., Meisinger, C., Guiard, B., Rehling, P., and Pfanner, N. (2003) A J-protein is an essential subunit of the presequence translocase-associated protein import motor of mitochondria. *J Cell Biol* **163**, 707-713
14. Hawlitschek, G., Schneider, H., Schmidt, B., Tropschug, M., Hartl, F. U., and Neupert, W. (1988) Mitochondrial protein import: identification of processing peptidase and of PEP, a processing enhancing protein. *Cell* **53**, 795-806
15. Rehling, P., Model, K., Brandner, K., Kovermann, P., Sickmann, A., Meyer, H. E., Kuhlbrandt, W., Wagner, R., Truscott, K. N., and Pfanner, N. (2003) Protein insertion into the mitochondrial inner membrane by a twin-pore translocase. *Science* **299**, 1747-1751
16. Duncan, O., Murcha, M. W., and Whelan, J. (2013) Unique components of the plant mitochondrial protein import apparatus. *Biochim Biophys Acta* **1833**, 304-313
17. Lister, R., Carrie, C., Duncan, O., Ho, L. H., Howell, K. A., Murcha, M. W., and Whelan, J. (2007) Functional definition of outer membrane proteins involved in preprotein import into mitochondria. *Plant Cell* **19**, 3739-3759
18. Rimmer, K. A., Foo, J. H., Ng, A., Petrie, E. J., Shilling, P. J., Perry, A. J., Mertens, H. D., Lithgow, T., Mulhern, T. D., and Gooley, P. R. (2011) Recognition of mitochondrial targeting sequences by the import receptors Tom20 and Tom22. *J Mol Biol* **405**, 804-818

19. Macasev, D., Whelan, J., Newbigin, E., Silva-Filho, M. C., Mulhern, T. D., and Lithgow, T. (2004) Tom22', an 8-kDa trans-site receptor in plants and protozoans, is a conserved feature of the TOM complex that appeared early in the evolution of eukaryotes. *Mol Biol Evol* **21**, 1557-1564
20. Pusnik, M., Schmidt, O., Perry, A. J., Oeljeklaus, S., Niemann, M., Warscheid, B., Lithgow, T., Meisinger, C., and Schneider, A. (2011) Mitochondrial preprotein translocase of trypanosomatids has a bacterial origin. *Curr Biol* **21**, 1738-1743
21. Mani, J., Meisinger, C., and Schneider, A. (2016) Peeping at TOMs-Diverse Entry Gates to Mitochondria Provide Insights into the Evolution of Eukaryotes. *Mol Biol Evol* **33**, 337-351
22. Zarsky, V., Tachezy, J., and Dolezal, P. (2012) Tom40 is likely common to all mitochondria. *Curr Biol* **22**, R479-481
23. Mani, J., Desy, S., Niemann, M., Chanfon, A., Oeljeklaus, S., Pusnik, M., Schmidt, O., Gerbeth, C., Meisinger, C., Warscheid, B., and Schneider, A. (2015) Mitochondrial protein import receptors in Kinetoplastids reveal convergent evolution over large phylogenetic distances. *Nat Commun* **6**, 6646
24. Pusnik, M., Mani, J., Schmidt, O., Niemann, M., Oeljeklaus, S., Schnarwiler, F., Warscheid, B., Lithgow, T., Meisinger, C., and Schneider, A. (2012) An essential novel component of the noncanonical mitochondrial outer membrane protein import system of trypanosomatids. *Mol Biol Cell* **23**, 3420-3428
25. Gentle, I. E., Perry, A. J., Alcock, F. H., Likic, V. A., Dolezal, P., Ng, E. T., Purcell, A. W., McConnville, M., Naderer, T., Chanez, A. L., Charriere, F., Aschinger, C., Schneider, A., Tokatlidis, K., and Lithgow, T. (2007) Conserved motifs reveal details of ancestry and structure in the small TIM chaperones of the mitochondrial intermembrane space. *Mol Biol Evol* **24**, 1149-1160
26. Singha, U. K., Peprah, E., Williams, S., Walker, R., Saha, L., and Chaudhuri, M. (2008) Characterization of the mitochondrial inner membrane protein translocator Tim17 from *Trypanosoma brucei*. *Mol Biochem Parasitol* **159**, 30-43
27. Doggett, J. S., Nilsen, A., Forquer, I., Wegmann, K. W., Jones-Brando, L., Yolken, R. H., Bordon, C., Charman, S. A., Katneni, K., Schultz, T., Burrows, J. N., Hinrichs, D. J., Meunier, B., Carruthers, V. B., and Riscoe, M. K. (2012) Endochin-like quinolones are highly efficacious against acute and latent experimental toxoplasmosis. *Proc Natl Acad Sci U S A* **109**, 15936-15941
28. Phillips, M. A., Gujjar, R., Malmquist, N. A., White, J., El Mazouni, F., Baldwin, J., and Rathod, P. K. (2008) Triazolopyrimidine-based dihydroorotate dehydrogenase inhibitors with potent and selective activity against the malaria parasite Plasmodium falciparum. *J Med Chem* **51**, 3649-3653
29. Srivastava, I. K., Rottenberg, H., and Vaidya, A. B. (1997) Atovaquone, a broad spectrum antiparasitic drug, collapses mitochondrial membrane potential in a malarial parasite. *J Biol Chem* **272**, 3961-3966
30. Alcock, F., Webb, C. T., Dolezal, P., Hewitt, V., Shingu-Vasquez, M., Likic, V. A., Traven, A., and Lithgow, T. (2012) A small Tim homohexamer in the relict mitochondrion of *Cryptosporidium*. *Mol Biol Evol* **29**, 113-122
31. Deponte, M., Hoppe, H. C., Lee, M. C., Maier, A. G., Richard, D., Rug, M., Spielmann, T., and Przyborski, J. M. (2012) Wherever I may roam: protein and membrane trafficking in *P. falciparum*-infected red blood cells. *Mol Biochem Parasitol* **186**, 95-116
32. van Dooren, G. G., Stimmler, L. M., and McFadden, G. I. (2006) Metabolic maps and functions of the *Plasmodium* mitochondrion. *FEMS Microbiol Rev* **30**, 596-630
33. Hell, K., Neupert, W., and Stuart, R. A. (2001) Oxa1p acts as a general membrane insertion machinery for proteins encoded by mitochondrial DNA. *EMBO J* **20**, 1281-1288
34. Chacinska, A., Pfannschmidt, S., Wiedemann, N., Kozjak, V., Sanjuan Szklarz, L. K., Schulze-Specking, A., Truscott, K. N., Guiard, B., Meisinger, C., and Pfanner, N. (2004) Essential role of

Mia40 in import and assembly of mitochondrial intermembrane space proteins. *EMBO J* **23**, 3735-3746
35. Sheiner, L., Fellows, J. D., Ovciarikova, J., Brooks, C. F., Agrawal, S., Holmes, Z. C., Bietz, I., Flinner, N., Heiny, S., Mirus, O., Przyborski, J. M., and Striepen, B. (2015) *Toxoplasma gondii* Toc75 Functions in Import of Stromal but not Peripheral Apicoplast Proteins. *Traffic* **16**, 1254-1269
36. Ahting, U., Thun, C., Hegerl, R., Typke, D., Nargang, F. E., Neupert, W., and Nussberger, S. (1999) The TOM core complex: the general protein import pore of the outer membrane of mitochondria. *J Cell Biol* **147**, 959-968
37. Gubbels, M. J., Li, C., and Striepen, B. (2003) High-throughput growth assay for *Toxoplasma gondii* using yellow fluorescent protein. *Antimicrob Agents Chemother* **47**, 309-316
38. van Dooren, G. G., Tomova, C., Agrawal, S., Humbel, B. M., and Striepen, B. (2008) *Toxoplasma gondii* Tic20 is essential for apicoplast protein import. *Proc Natl Acad Sci U S A* **105**, 13574-13579
39. Banaszynski, L. A., Chen, L. C., Maynard-Smith, L. A., Ooi, A. G., and Wandless, T. J. (2006) A rapid, reversible, and tunable method to regulate protein function in living cells using synthetic small molecules. *Cell* **126**, 995-1004
40. Yano, M., Hoogenraad, N., Terada, K., and Mori, M. (2000) Identification and functional analysis of human Tom22 for protein import into mitochondria. *Mol Cell Biol* **20**, 7205-7213
41. Sheiner, L., Demerly, J. L., Poulsen, N., Beatty, W. L., Lucas, O., Behnke, M. S., White, M. W., and Striepen, B. (2011) A systematic screen to discover and analyze apicoplast proteins identifies a conserved and essential protein import factor. *PLoS Pathog* **7**, e1002392
42. Cavalier-Smith, T. (2006) Origin of mitochondria by intracellular enslavement of a photosynthetic purple bacterium. *Proc Biol Sci* **273**, 1943-1952
43. Dolezal, P., Dagley, M. J., Kono, M., Wolynec, P., Likic, V. A., Foo, J. H., Sedinova, M., Tachezy, J., Bachmann, A., Bruchhaus, I., and Lithgow, T. (2010) The essentials of protein import in the degenerate mitochondrion of *Entamoeba histolytica*. *PLoS Pathog* **6**, e1000812
44. Dekker, P. J., Ryan, M. T., Brix, J., Muller, H., Honlinger, A., and Pfanner, N. (1998) Preprotein translocase of the outer mitochondrial membrane: molecular dissection and assembly of the general import pore complex. *Mol Cell Biol* **18**, 6515-6524
45. Werhahn, W., Niemeyer, A., Jansch, L., Kruft, V., Schmitz, U. K., and Braun, H. (2001) Purification and characterization of the preprotein translocase of the outer mitochondrial membrane from *Arabidopsis*. Identification of multiple forms of TOM20. *Plant Physiol* **125**, 943-954
46. Paschen, S. A., Waizenegger, T., Stan, T., Preuss, M., Cyrklaff, M., Hell, K., Rapaport, D., and Neupert, W. (2003) Evolutionary conservation of biogenesis of beta-barrel membrane proteins. *Nature* **426**, 862-866
47. Wiedemann, N., Kozjak, V., Chacinska, A., Schonfisch, B., Rospert, S., Ryan, M. T., Pfanner, N., and Meisinger, C. (2003) Machinery for protein sorting and assembly in the mitochondrial outer membrane. *Nature* **424**, 565-571
48. Becker, T., Wenz, L. S., Thornton, N., Stroud, D., Meisinger, C., Wiedemann, N., and Pfanner, N. (2011) Biogenesis of mitochondria: dual role of Tom7 in modulating assembly of the preprotein translocase of the outer membrane. *J Mol Biol* **405**, 113-124
49. Yamano, K., Tanaka-Yamano, S., and Endo, T. (2010) Tom7 regulates Mdm10-mediated assembly of the mitochondrial import channel protein Tom40. *J Biol Chem* **285**, 41222-41231
50. Huynh, M. H., and Carruthers, V. B. (2009) Tagging of endogenous genes in a *Toxoplasma gondii* strain lacking Ku80. *Eukaryot Cell* **8**, 530-539
51. Meissner, M., Schluter, D., and Soldati, D. (2002) Role of *Toxoplasma gondii* myosin A in powering parasite gliding and host cell invasion. *Science* **298**, 837-840

52. Striepen, B., and Soldati, D. (2007) Genetic manipulation of *Toxoplasma gondii*. in *Toxoplasma gondii. The Model Apicomplexan - Perspectives and Methods* (Weiss, L. D., and Kim, K. eds.), Elsevier, London. pp 391-415
53. Glaser, S., van Dooren, G. G., Agrawal, S., Brooks, C. F., McFadden, G. I., Striepen, B., and Higgins, M. K. (2012) Tic22 is an essential chaperone required for protein import into the apicoplast. *J Biol Chem* **287**, 39505-39512
54. Messina, M., Niesman, I., Mercier, C., and Sibley, L. D. (1995) Stable DNA transformation of *Toxoplasma gondii* using phleomycin selection. *Gene* **165**, 213-217
55. Katris, N. J., van Dooren, G. G., McMillan, P. J., Hanssen, E., Tilley, L., and Waller, R. F. (2014) The apical complex provides a regulated gateway for secretion of invasion factors in *Toxoplasma*. *PLoS Pathog* **10**, e1004074
56. Agrawal, S., van Dooren, G. G., Beatty, W. L., and Striepen, B. (2009) Genetic evidence that an endosymbiont-derived endoplasmic reticulum-associated protein degradation (ERAD) system functions in import of apicoplast proteins. *J Biol Chem* **284**, 33683-33691
57. Mazumdar, J., E.H., W., Masek, K., C.A., H., and Striepen, B. (2006) Apicoplast fatty acid synthesis is essential for organelle biogenesis and parasite survival in *Toxoplasma gondii*. *Proc Natl Acad Sci U S A* **103**, 13192-13197
58. van Dooren, G. G., Reiff, S. B., Tomova, C., Meissner, M., Humbel, B. M., and Striepen, B. (2009) A novel dynamin-related protein has been recruited for apicoplast fission in *Toxoplasma gondii*. *Curr Biol* **19**, 267-276
59. Alexandrov, A., Vignali, M., LaCount, D. J., Quartley, E., de Vries, C., De Rosa, D., Babulski, J., Mitchell, S. F., Schoenfeld, L. W., Fields, S., Hol, W. G., Dumont, M. E., Phizicky, E. M., and Grayhack, E. J. (2004) A facile method for high-throughput co-expression of protein pairs. *Mol Cell Proteomics* **3**, 934-938
60. Bastin, P., Bagherzadeh, Z., Matthews, K. R., and Gull, K. (1996) A novel epitope tag system to study protein targeting and organelle biogenesis in *Trypanosoma brucei*. *Mol Biochem Parasitol* **77**, 235-239
61. Carey, K. L., Donahue, C. G., and Ward, G. E. (2000) Identification and molecular characterization of GRA8, a novel, proline-rich, dense granule protein of *Toxoplasma gondii*. *Mol Biochem Parasitol* **105**, 25-37
62. Tonkin, C. J., van Dooren, G. G., Spurck, T. P., Struck, N. S., Good, R., Handman, E., Cowman, A. F., and McFadden, G. I. (2004) Localization of organellar proteins in *Plasmodium falciparum* using a novel set of transfection vectors and a new immunofluorescence fixation method. *Mol Biochem Parasitol* **137**, 13-21

FIGURE LEGENDS

FIGURE 1. Localization of putative mitochondrial import proteins in *T. gondii*. (A, B, D, F, H, J, L, and N) Target proteins are labelled in green, and, in all cases, they co-localize with a mitochondrial marker (either RFP fused to the mitochondrial matrix-targeting leader sequence of *Tg*Hsp60 or anti-Tom40 antibodies; red). Scale bars are 2 µm. (C, E, G, I, K, and M) Western blots of each protein are shown to the right of each panel. For the *Tg*Tom40 western blot, protein extracts from wild type (WT) and the HA-tagged *Tg*Tom40 strain were probed with anti-*Tg*Tom40 antibodies. Our transfection experiments did not produce tagged *Tg*Pam18 in sufficient quantity to detect by western blotting. O. Schematic depicting the putative composition of the TOM, SAM, TIM23, PAM and TIM22 complexes in *T. gondii*. Proteins localised in this study are depicted in light green, proteins identified bioinformatically are depicting in dark green, and notable proteins without homologues in *T. gondii* are depicted in gray. OMM, outer mitochondrial membrane; IMM, inner mitochondrial membrane.

FIGURE 2. *Tg*Tom22 is a mitochondrial membrane protein with homology to Tom22 proteins from other eukaryotes. (A) Multiple protein sequence alignment of *Tg*Tom22 with homologues from *P. falciparum* (*Pf*Tom22), humans (*Hs*Tom22), *A. thaliana* (*At*Tom22), and *S. cerevisiae* (*Sc*Tom22). Transmembrane domains of each protein (predicted using TMHMM; http://www.cbs.dtu.dk/services/TMHMM/) are highlighted by a box. (B) An immunofluorescence assay demonstrating co-localization of HA-Tom22 protein (green) with the mitochondrion marker Tom40 (red). Scale bar is 2 µm. A western blot analysis of HA-Tom22, probed with anti-HA antibodies reveals a protein with a mass of 10 kDa. (C) A western blot analysis of HA-Tom22-expressing parasites, where proteins were extracted in 1% Triton X-100 (TX-100) or in sodium carbonate (Na_2CO_3) at pH 11.5. HA-Tom22 partitions into the pellet phase of the Na_2CO_3 extraction, much like the integral mitochondrial membrane protein Tom40, and unlike the soluble mitochondrial matrix protein ATP synthase β subunit, which partitions predominantly into the supernatant (S/N) phase.

FIGURE 3. Generation of mutant parasite strains. (A) Schematic describing knockout of the native *Tg*Tom22 gene. The native *Tg*Tom22 locus (orange) was replaced with a chloramphenicol acetyl transferase (CAT) selectable marker (blue), in a background strain expressing an ATc-regulatable copy of *Tg*Tom22 (not shown). (B) PCR screen of 12 parasite clones transfected with the *Tg*Tom22 knockout construct with primers 21 and 22. The primer pair will produce a band of 0.8 kb if the native gene is present, and a band of 1.6 kb when the regulatable copy of *Tg*Tom22 is present. Clones 3 and 5–11 lack the native gene, indicating successful knockout of the *Tg*Tom22 native locus in these parasites. (C) Schematic describing replacement of the native *Tg*Tom7 promoter with an ATc-regulated promoter (t7s4) and 5' HA tag. The TATi/Δ*ku80* parasite strain was transfected with a vector containing 5' and 3' flanks of the *Tg*Tom7 gene, the t7s4 ATc-regulated promoter, a 5' HA tag, and a pyrimethamine-resistant *T. gondii* dihydrofolate reductase (DHFR) selectable marker. (D) PCR screen of six parasite clones transfected with the promoter replacement vector, and screened with primer pairs 31 and 32 to detect the native *Tg*Tom7 locus (top) or primer pairs 32 and 33 to detect the modified locus (bottom). DNA from wild type (WT) TATi/Δ*ku80* parasites was used as a control. Clones 1, 3 and 4 lack the band corresponding to the presence of the native gene, but harbor the band corresponding to the modified locus, indicating successful promoter replacement at the *Tg*Tom7 locus in these parasites.

FIGURE 4. *T. gondii* harbors a TOM complex of ~400 kDa that contains *Tg*Tom40 and *Tg*Tom22. (A). Western blot probing *Tg*Tom40 proteins separated by BN-PAGE extracted in 0.5% (w/v) digitonin, 1% (w/v) digitonin, 1% (w/v) dodecylmaltoside (DDM), 1% (w/v) octyl b-D-glucopyranoside (OGP) and 1% (w/v) TX-100. (B) Western blot probing *Tg*Tom40, HA-Tom22 and Sam50-cmyc proteins separated by BN-PAGE in a first dimension and SDS-PAGE in a second dimension. (C) Western blots of immunoprecipitated parasite proteins extracted in 0.5% digitonin and pulled down with anti-Tom40 antibodies (left) or anti-HA antibodies (right). Western blots were probed for *Tg*Tom40 (top), HA-Tom22

(middle), and Sam50-cmyc (bottom). Total proteins, unbound proteins and bound proteins were loaded for each experiment, and each lane contains proteins extracted from an equivalent number of parasites. The heavy chain of anti-Tom40 antibodies was detectable in the anti-Tom40 western blot.

FIGURE 5. *Tg*Tom22 is essential for parasite growth. (A) Western blot of rTom22/Δ*tom22* parasites grown for 0-2 days on ATc and probed with anti-HA antibodies to detect HA-Tom22 protein or anti-GRA8 antibodies as a loading control. (B-C) Fluorescence growth assays of (B) *Tg*Tom22 knockdown (rTom22/Δ*tom22*) and (C) *Tg*Tom22 complemented (rTom22/Δ*tom22*/Tom22wt) strains. Parasites were grown in the absence (black) or presence (red) of ATc for 0 to 8 days. Error bars represent the standard deviation of three technical replicates.

FIGURE 6. *Tg*Tom22 is essential for mitochondrial protein import and functions in assembly of the TOM complex. (A) Western blots of HA-Tom22 parasites expressing cmyc-tagged mouse DHFR fused to the mitochondrial-targeting leader sequence of *Tg*Hsp60 ($Hsp60_L$-DHFR-cmyc). Parasites were grown for 0 to 3 days in ATc and protein extracts were probed with anti-HA, anti-Hsp60, anti-cmyc, anti-*Tg*Tom40 and anti-GRA8 antibodies as a loading control. Precursor (p) and mature (m) forms of the Hsp60 and $Hsp60_L$-DHFR-cmyc protein are indicated. This experiment was performed in three biological replicates, and a representative experiment is shown. (B) Import of radiolabelled $Hsp60_L$-DHFR-cmyc protein into the mitochondrion of rTom22/Δ*tom22* parasites grown for 0 (no ATc) or 2 (d2 +ATc) days on ATc. Intracellular parasites were incubated for 10, 30 and 60 mins in growth medium containing [^{35}S]-labelled cysteine and methionine. Proteins were extracted in detergent and $Hsp60_L$-DHFR-cmyc protein purified by immunoprecipitation before separation by SDS-PAGE. Precursor (p$Hsp60_L$-DHFR-cmyc) and mature (m$Hsp60_L$-DHFR-cmyc) isoforms of the $Hsp60_L$-DHFR-cmyc protein were detected. This experiment was performed in two biological replicates, and a representative experiment is shown. (C) Anti-Tom40 western blot of proteins extracted from rTom22/Δ*tom22* parasites grown for 0–3 days in ATc and separated by BN-PAGE. (D) Western blot of proteins extracted from rTom22/Δ*tom22* parasites grown in the absence (top) or presence of ATc for 2 days (bottom). Proteins were separated by BN-PAGE in a first dimension and SDS-PAGE in a second dimension, then probed with anti-Tom40 antibodies. (E-F) Fluorescence growth assays of (E) rTom22/Δ*tom22* parasites and (F) rTom22/Δ*tom22* complemented with DD-tagged wild type *Tg*Tom22 (rTom22/Δ*tom22*/DD-Tom22wt), grown in the absence (black) or presence (red) of ATc, or in the presence of ATc and Shld1 (blue). Note that the red +ATc line in E is not visible behind the blue +ATc/+Shld1 line. Error bars represent the standard deviation of three technical replicates. (G) Anti-Tom40 western blot of proteins extracted from rTom22/Δ*tom22*/DD-Tom22wt parasites separated by BN-PAGE. Parasites were grown in the absence of ATc, or in the presence of ATc for 2 days in ATc. Parasites grown in ATc were also grown for 0–48 hours in Shld1.

FIGURE 7. *Tg*Tom7 is a mitochondrial protein and a constituent of the TOM complex. (A) Multiple protein sequence alignment of the long and short isoforms of *Tg*Tom7 with homologues from *N. caninum* (*Nc*Tom7), *P. falciparum* (*Pf*Tom7), *S. cerevisiae* (*Sc*Tom7), *A. thaliana* (*At*Tom7-1) and humans (*Hs*Tom7). Transmembrane domains of each protein (predicted using TMHMM) are highlight by a box. (B) An immunofluorescence assay demonstrating co-localization of a HA-tagged version of the short isoform of *Tg*Tom7 (HA_3-Tom7; green) with the mitochondrial marker Tom40 (red). Scale bar is 2 µm. (C) A western blot analysis of HA_3-Tom7, probed with anti-HA antibodies reveals a protein of 11 kDa. (D) Western blot of proteins extracted from the TATi/Δ*ku80*/rTom7 parasite strain and separated by BN-PAGE in a first dimension and SDS-PAGE in a second dimension. Blots were probed with anti-Tom40 antibodies (top) and anti-HA antibodies to detect HA_3-Tom7 protein (bottom). (E) Western blots of parasite proteins extracted from TATi/Δ*ku80*/rTom7 strain parasites in 0.5% digitonin, immunoprecipitated with anti-Tom40 antibodies, and separated by SDS-PAGE. Blots were probed with anti-Tom40 antibodies (top) and anti-HA antibodies (bottom). Total proteins, unbound proteins and bound proteins were loaded for each experiment, and each lane contains proteins extracted from an

equivalent number of parasites. The heavy chain of anti-Tom40 antibodies was detectable in the anti-Tom40 western blot.

FIGURE 8. *Tg*Tom7 is important for parasite growth, mitochondrial protein import, and TOM complex assembly. (A) Western blot of proteins extracted from TATi/Δ*ku80*/rTom7 grown for 0–3 days in ATc. Blots were probed with antibodies against HA_3-Tom7, *Tg*GRA8 (loading control), *Tg*Tom40 and *Tg*Hsp60. Precursor and mature forms of *Tg*Hsp60 are indicated. This experiment was performed in three biological replicates, and a representative experiment is shown. (B-D) Fluorescence growth assays of (B) TATi/Δ*ku80* parental control, (C) *Tg*Tom7 knockdown (TATi/Δ*ku80*/rTom7) and (D) *Tg*Tom7 complemented (TATi/Δ*ku80*/rTom7/Tom7wt) strains. Parasites were grown in the absence (black) or presence (red) of ATc for 0 to 6 days. Error bars represent the standard deviation of three technical replicates. (E) Anti-Tom40 western blot of proteins extracted from TATi/Δ*ku80*/rTom7 parasites grown for 0–3 days in ATc and separated by BN-PAGE. (F) Western blot of proteins extracted from TATi/Δ*ku80*/rTom7 parasites grown in the absence (top) or presence of ATc for 2 days (bottom). Proteins were separated by BN-PAGE in a first dimension and SDS-PAGE in a second dimension, and probed with anti-Tom40 antibodies.

Table 1. Primers used for generating vectors and screening parasite strains

No.	Primer name	Primer sequence
1	*Tg*Tom40 3'rep fwd	5'-TACTTCCAATCCAATTTAGCTAAGCTGCAATTGGGAGGCG
2	*Tg*Tom40 3'rep rvs	5'-TCCTCCACTTCCAATTTTAGCCATCGGAGGAGGCTGTTCC
3	*Tg*Sam50 orf fwd	5'-GATCAGATCTACTAGTAAAATGGCGGGGTCAGCTCCTACC
4	*Tg*Sam50 orf rvs	5'-CAGTCCTAGGCTCGGGGAGTCTTCCAGAAGAAAGAC
5	*Tg*Tim22 3'rep fwd	5'-GATCAGATCTACTAGTCAGATGCGGCAGCAATATCGGAAC
6	*Tg*Tim22 3'rep rvs	5'-CAGTCCTAGGCGCTCCCATGTTTCCAAAAGGCTG
7	*Tg*Tim23 3'rep fwd	5'-GTCAAGATCTACTAGTAAGGCAGGCGCTCAGCTTGGC
8	*Tg*Tim23 3'rep rvs	5'-CAGTCCTAGGGACGTACTTGCGAAGGTACTGG
9	*Tg*Tim50 3'rep fwd	5'-TACTTCCAATCCAATTTAGCAAATCGTGCTTCCTTGTGGTTG
10	*Tg*Tim50 3'rep rvs	5'-TCCTCCACTTCCAATTTTAGCGGCCTTTTCCCACTTTTGTCTCTG
11	*Tg*Pam18 orf fwd	5'-AGATCTACTAGTAAAATGTGGGCACTGGCCTGCTTCCTG
12	*Tg*Pam18 orf rvs	5'-CCTAGGCCGCCGGCTGTCCTTCAGCAGCTTC
13	*Tg*MPPβ 3'rep fwd	5'-TACTTCCAATCCAATTTAGCGAGTTTCAAATCAGTTCCCTCTTCAG
14	*Tg*MPPβ 3'rep rvs	5'- TCCTCCACTTCCAATTTTAGCCTTGCCGACGCCCGCGGC
15	*Tg*Tom22 orf fwd	5'- TCCCCCCGGGGCTAGCATGGGGAACCTCCTGTCCTCGC
16	*Tg*Tom 22 orf rvs	5'- ATCGGATATCGACGTCTCACACCGAAGGAGTCGCC
17	*Tg*Tom22 5'flank fwd	5'- ACTAGTCTTAGGGGTGTGCAGATTGGTGCCTT
18	*Tg*Tom22 5'flank rvs	5'- AGATCTTTTGGAGGAAACAGGAGAGCGAGTGAC
19	*Tg*Tom22 3'flank fwd	5'- GTCGACGGGGACCTCGAATGCCGTTTGAGGTAT
20	*Tg*Tom22 3'flank rvs	5'- GGGCCCGGCACGCCTCATTTTCCGGTCTTG
21	*Tg*Tom22 screen fwd	5'-TTTCTCGGCTGGTTTCTTAG
22	*Tg*Tom22 screen fwd	5'-GGGCGAGATTGACGAAGC
23	*Tg*Tom22 comp fwd	5'-GATCCCCGGGCTTAAGCCATGGCATATGGGGAACCTCCTGTCCTCG
24	*Tg*Tom22 comp rvs	5'- GATCGACGTCTCACACCGAAGGAGTCGCCC
25	*Tg*Tom7 5'RACE	5'-CTGGAATAAGCTCGTCGGATCCAGAGTC
26	*Tg*Tom7 5'RACE nested	5'-CTCTCCCGTGTAGGCCAGGCCAAC
27	*Tg*Tom7 3'flank fwd	5'-GATCCCCGGGATGGGCCAGGTTTTGAGTCATTG
28	*Tg*Tom7 3'flank rvs	5'-CGATGCGGCCGCCAATCACCGAGTGGCGTTAATACC
29	*Tg*Tom7 5'flank fwd	5'- CGATGGGCCCCTATCTGTCGGACCCAACTACTCAAAC
30	*Tg*Tom7 5'flank rvs	5'-CGTAGGCGCGCCTAGTGCTTCCACAAATTGCTGTTGG
31	*Tg*Tom7 screen fwd	5'-CGTCGGTGGAATCTGCTG
32	*Tg*Tom7 screen fwd	5'-TACGTGCACCAGCAATGTC
33	t7s4 screen fwd	5'-AAGGGGACGCAGTTCTCGGA
34	*Tg*Tom7 comp fwd	5'-GATCCCATGGCCCGGGATGGGCCAGGTTTTGAGTCATTG
35	*Tg*Tom7 comp rvs	5'-GATCCAATTGTCAGTTGATGACAATTTTCTGGAA
36	*Tg*Tom40 Ab fwd	5'-GGGTCCTGGTTCGATGAAAACGTCTTCTCGCCATGAAGAGC
37	*Tg*Tom40 Ab rvs	5'-CTTGTTCGTGCTGTTTATTAGCCTGCCACGGCCATCCATTC

Figure 1

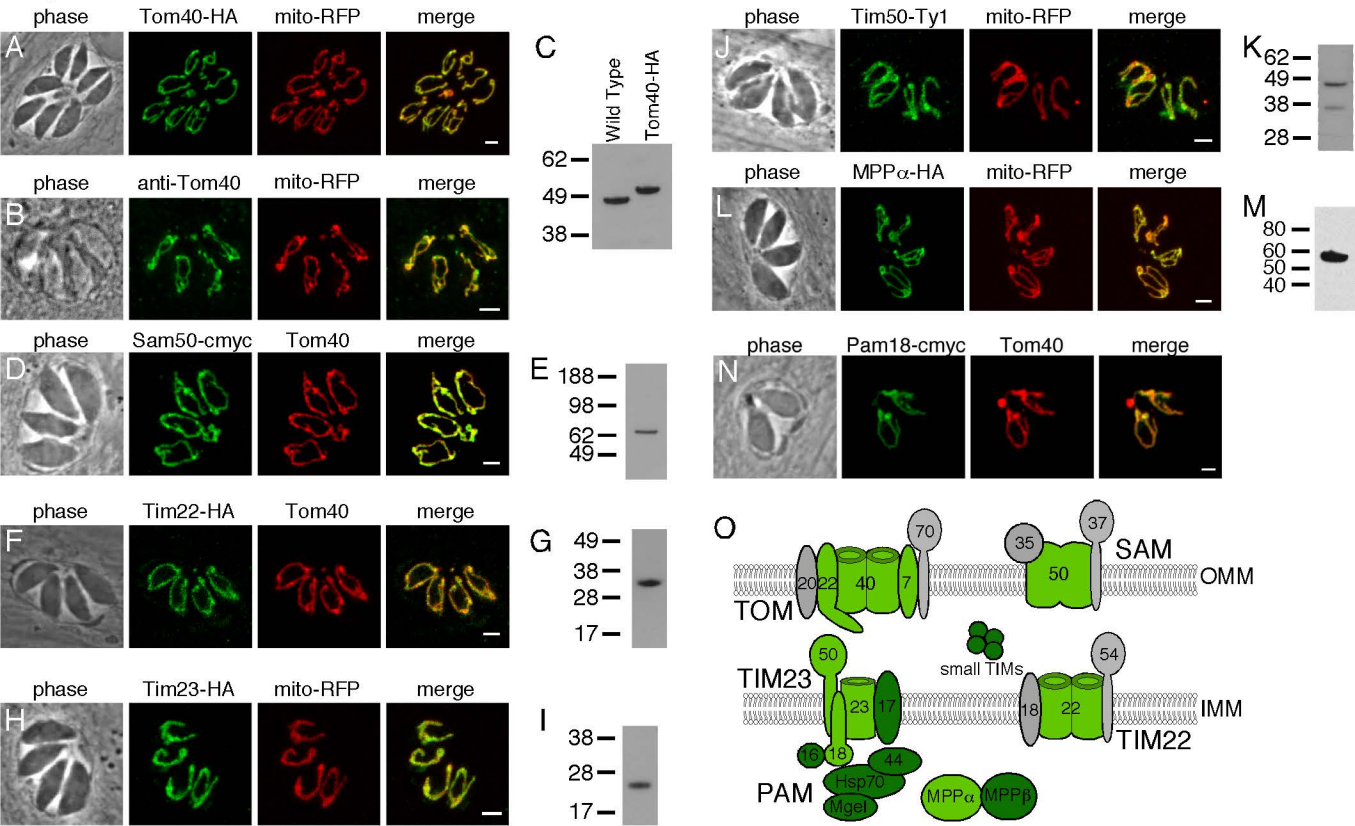
phase
Tom40-HA
mito-RFP
merge
A
B
anti-Tom40
D
Sam50-cmyc
Tom40
F
Tim22-HA
H
Tim23-HA
C
Wild Type
Tom40-HA
62
49
38
E
188
98
62
49
G
49
38
28
17
I
38
28
17
J
Tim50-Ty1
K
62
49
38
28
L
MPPα-HA
M
80
60
50
40
N
Pam18-cmyc
O
70
20
22
40
7
TOM
OMM
35
37
SAM
50
small TIMs
TIM23
50
23
17
16
18
44
Hsp70
Mge1
PAM
MPPα
MPPβ
IMM
54
18
22
TIM22

Figure 2

A.

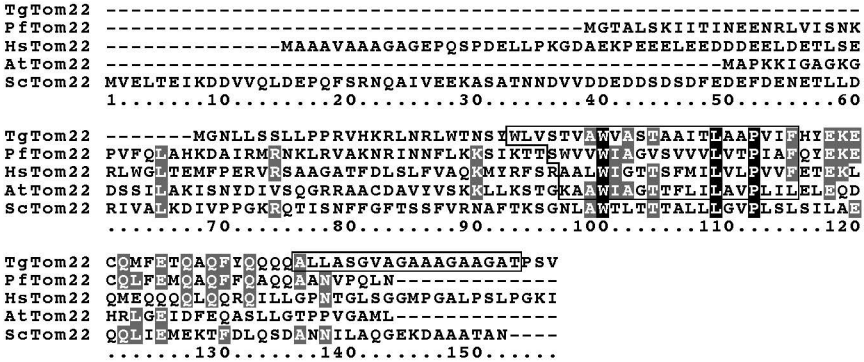
TgTom22
PfTom22
HsTom22
AtTom22
ScTom22
1.....10.....20.....30.....40.....50.....60
.....70.....80.....90.....100.....110.....120
.....130.....140.....150.....

B.

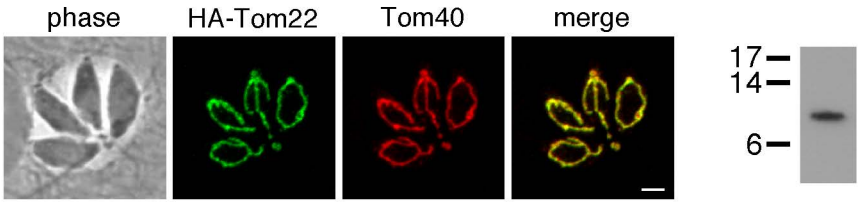
phase
HA-Tom22
Tom40
merge
17
14
6

C.

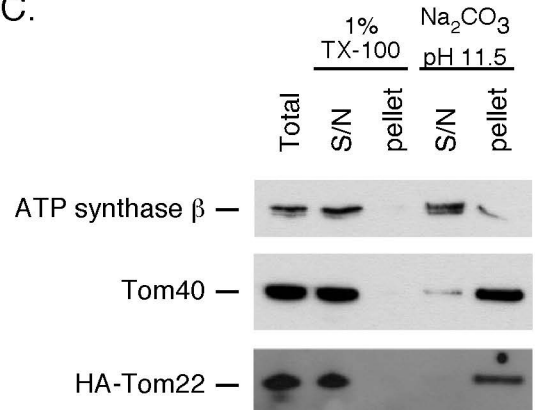
1% TX-100
Na2CO3 pH 11.5
Total
S/N
pellet
S/N
pellet
ATP synthase β
Tom40
HA-Tom22

Figure 3

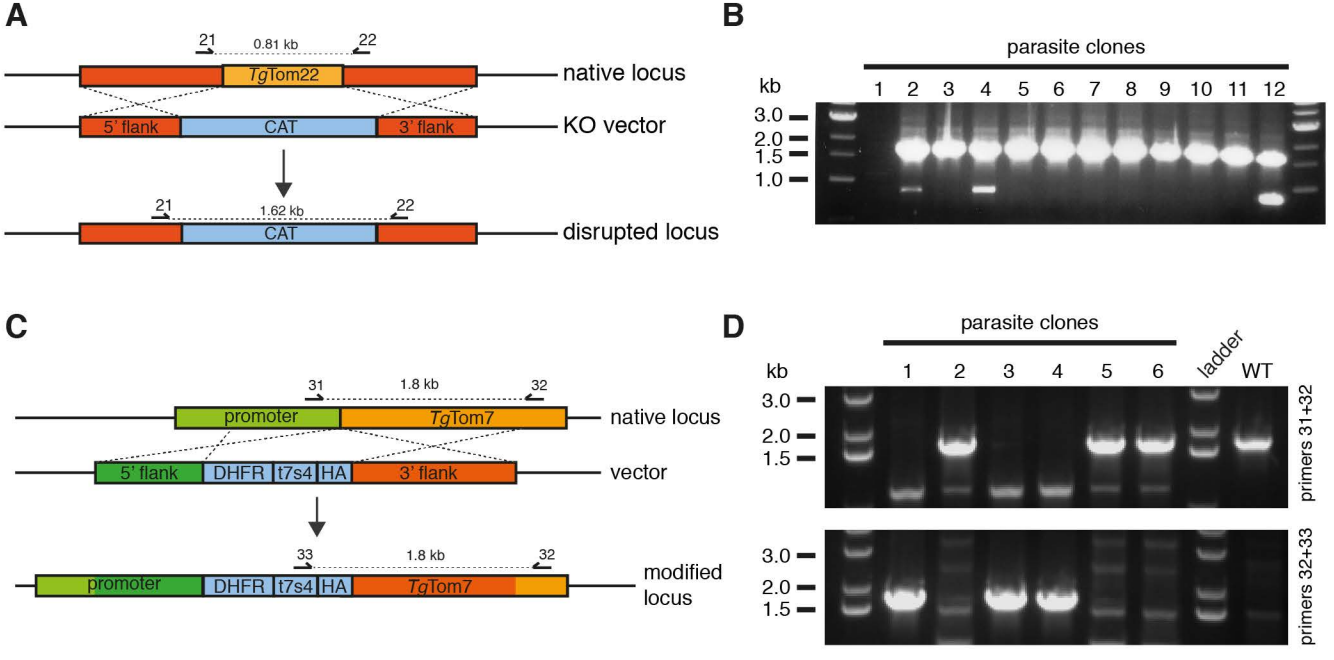
A
21
0.81 kb
22
native locus
TgTom22
5' flank
CAT
3' flank
KO vector
21
1.62 kb
22
CAT
disrupted locus
B
parasite clones
kb
1 2 3 4 5 6 7 8 9 10 11 12
3.0
2.0
1.5
1.0
C
31
1.8 kb
32
promoter
TgTom7
native locus
5' flank
DHFR
t7s4
HA
3' flank
vector
33
1.8 kb
32
promoter
DHFR
t7s4
HA
TgTom7
modified locus
D
parasite clones
kb
1 2 3 4 5 6
ladder
WT
3.0
2.0
1.5
primers 31+32
3.0
2.0
1.5
primers 32+33

Figure 4

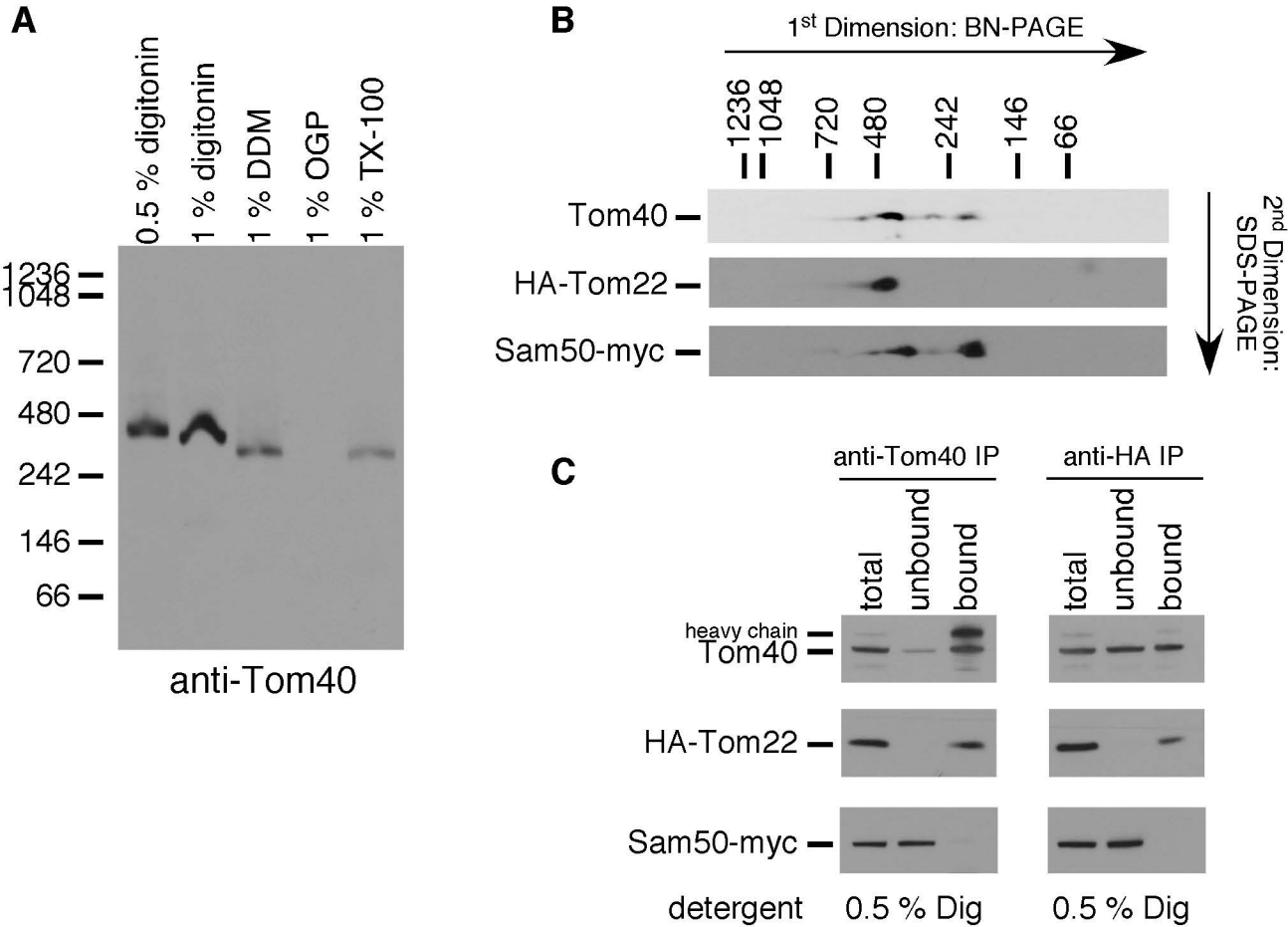
A
0.5 % digitonin
1 % digitonin
1 % DDM
1 % OGP
1 % TX-100
1236
1048
720
480
242
146
66
anti-Tom40
B
1st Dimension: BN-PAGE
1236
1048
720
480
242
146
66
Tom40
HA-Tom22
Sam50-myc
2nd Dimension: SDS-PAGE
C
anti-Tom40 IP
anti-HA IP
total
unbound
bound
total
unbound
bound
heavy chain
Tom40
HA-Tom22
Sam50-myc
detergent
0.5 % Dig
0.5 % Dig

Figure 5

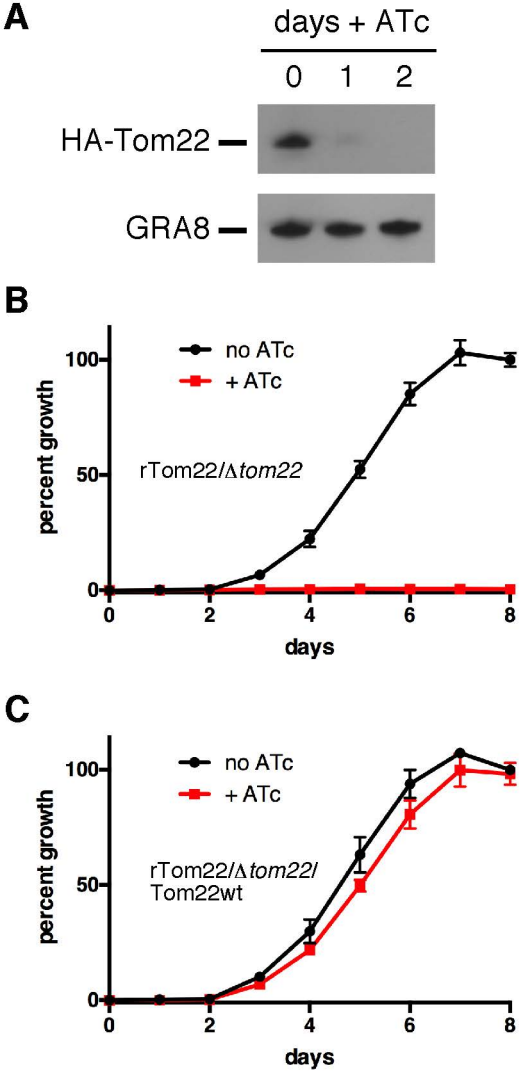
A
days + ATc
0 1 2
HA-Tom22
GRA8
B
no ATc
+ ATc
rTom22/Δtom22
percent growth
100
50
0
0 2 4 6 8
days
C
no ATc
+ ATc
rTom22/Δtom22/
Tom22wt
percent growth
100
50
0
0 2 4 6 8
days

Figure 6

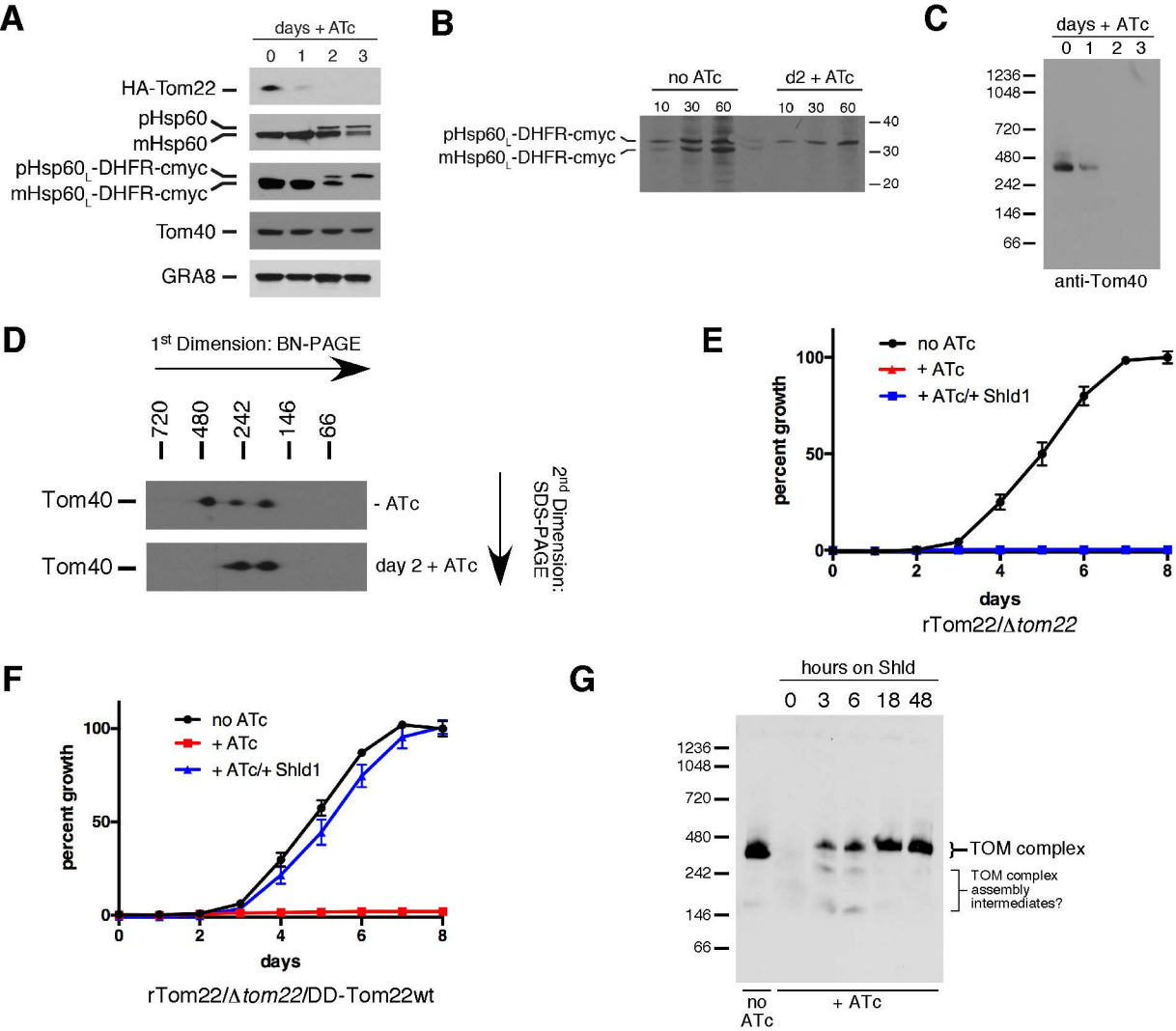
A
days + ATc
0 1 2 3
HA-Tom22
pHsp60
mHsp60
pHsp60L-DHFR-cmyc
mHsp60L-DHFR-cmyc
Tom40
GRA8
B
no ATc
d2 + ATc
10 30 60 10 30 60
pHsp60L-DHFR-cmyc
mHsp60L-DHFR-cmyc
40
30
20
C
days + ATc
0 1 2 3
1236
1048
720
480
242
146
66
anti-Tom40
D
1st Dimension: BN-PAGE
720 480 242 146 66
Tom40
- ATc
Tom40
day 2 + ATc
2nd Dimension: SDS-PAGE
E
no ATc
+ ATc
+ ATc/+ Shld1
percent growth
100
50
0
0 2 4 6 8
days
rTom22/Δtom22
F
no ATc
+ ATc
+ ATc/+ Shld1
percent growth
100
50
0
0 2 4 6 8
days
rTom22/Δtom22/DD-Tom22wt
G
hours on Shld
0 3 6 18 48
1236
1048
720
480
242
146
66
TOM complex
TOM complex assembly intermediates?
no ATc
+ ATc

Figure 7

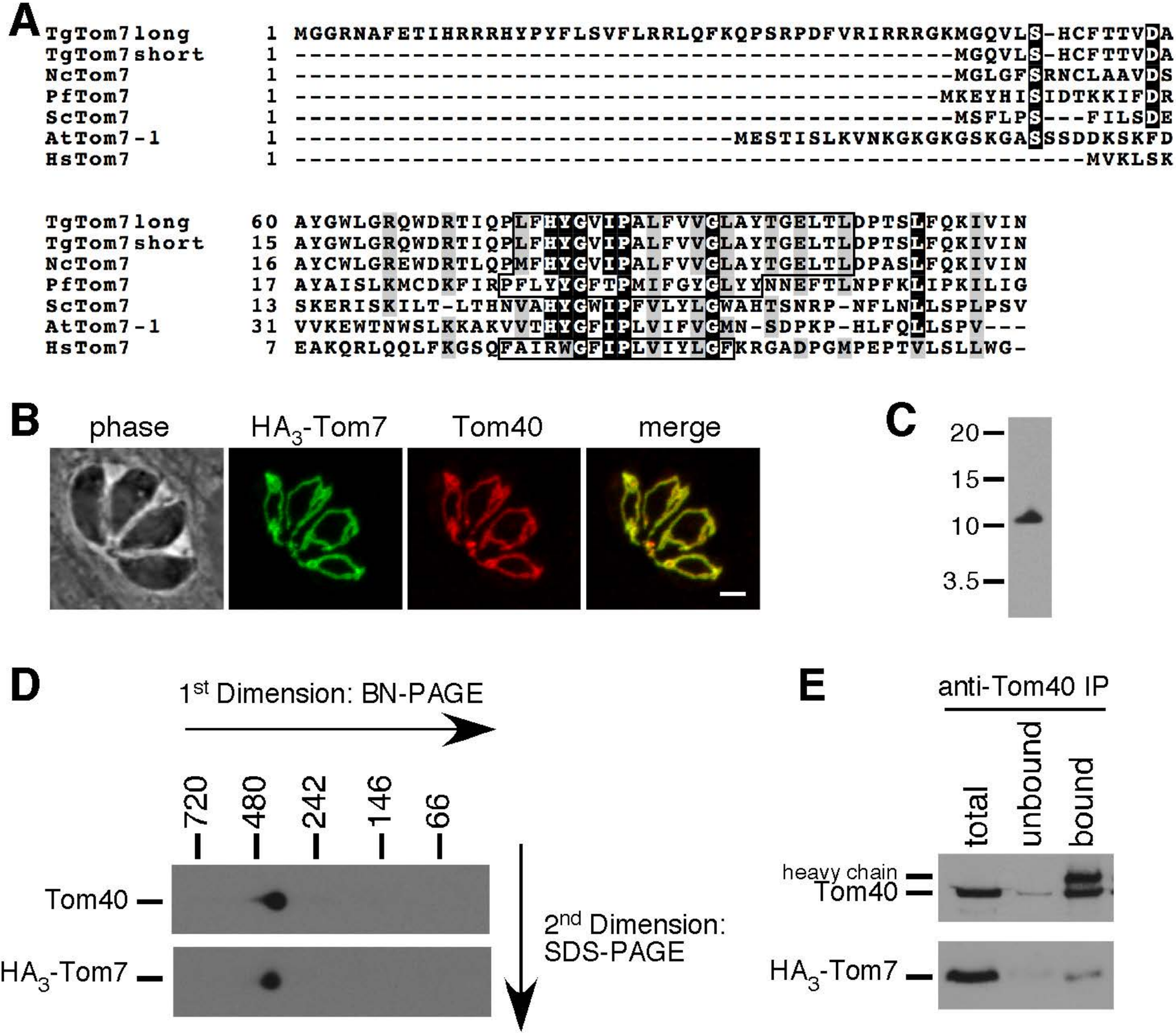
A
TgTom7long 1 MGGRNAFETIHRRRHYPYFLSVFLRRLQFKQPSRPDFVRIRRRGKMGQVLS-HCFTTVDA
TgTom7short 1 ----------MGQVLS-HCFTTVDA
NcTom7 1 ----------MGLGFSRNCLAAVDS
PfTom7 1 ----------MKEYHISIDTKKIFDR
ScTom7 1 ----------MSFLPS---FILSDE
AtTom7-1 1 ----------MESTISLKVNKGKGKGSKGASSSDDKSKFD
HsTom7 1 ----------MVKLSK
TgTom7long 60 AYGWLGRQWDRTIQPLFHYGVIPALFVVGLAYTGELTLDPTSLFQKIVIN
TgTom7short 15 AYGWLGRQWDRTIQPLFHYGVIPALFVVGLAYTGELTLDPTSLFQKIVIN
NcTom7 16 AYCWLGREWDRTLQPMFHYGVIPALFVVGLAYTGELTLDPASLFQKIVIN
PfTom7 17 AYAISLKMCDKFIRPFLYYGFTPMIFGYGLYYNNEFTLNPFKLIPKILIG
ScTom7 13 SKERISKILT-LTHNVAHYGWIPFVLYLGWAHTSNRP-NFLNLLSPLPSV
AtTom7-1 31 VVKEWTNWSLKKAKVVTHYGFIPLVIFVGMN-SDPKP-HLFQLLSPV---
HsTom7 7 EAKQRLQQLFKGSQFAIRWGFIPLVIYLGFKRGADPGMPEPTVLSLLWG-
B
phase
HA3-Tom7
Tom40
merge
C
20
15
10
3.5
D
1st Dimension: BN-PAGE
720
480
242
146
66
Tom40
HA3-Tom7
2nd Dimension:
SDS-PAGE
E
anti-Tom40 IP
total
unbound
bound
heavy chain
Tom40
HA3-Tom7

Figure 8

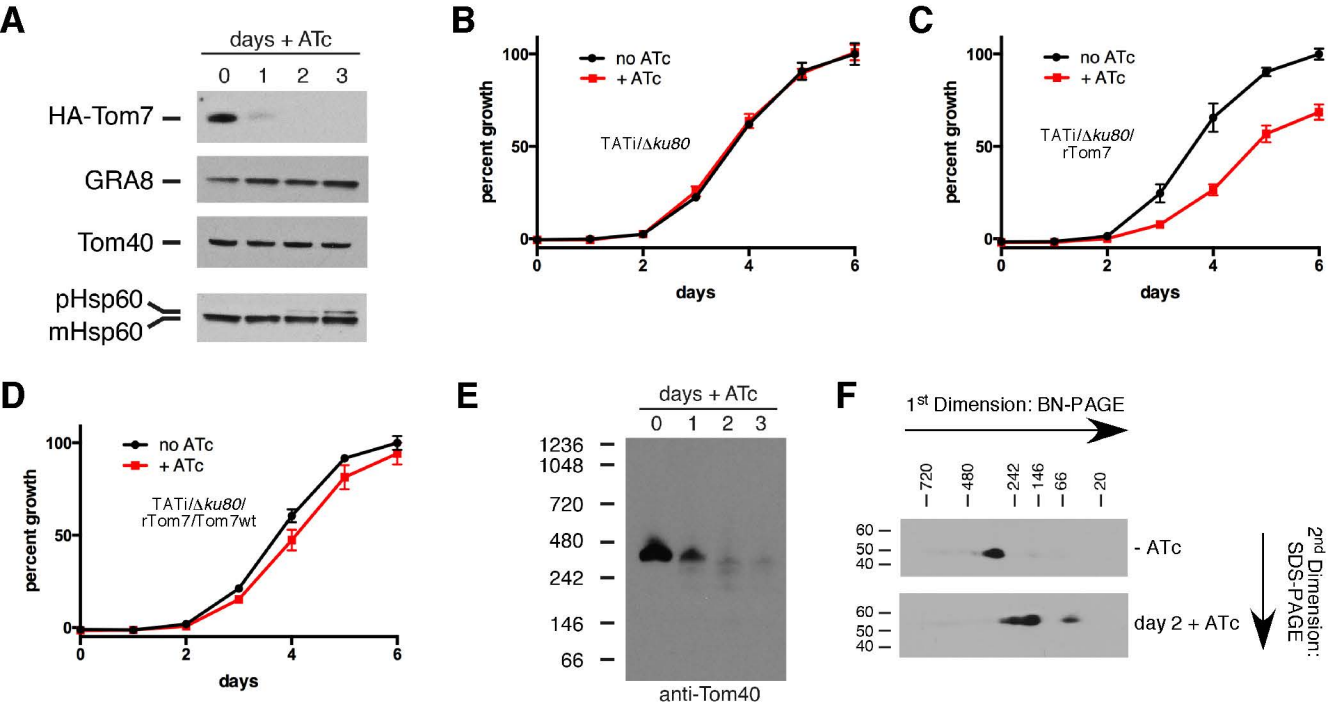
A
days + ATc
0 1 2 3
HA-Tom7
GRA8
Tom40
pHsp60
mHsp60
B
no ATc
+ ATc
TATi/Δku80
percent growth
days
C
no ATc
+ ATc
TATi/Δku80/
rTom7
percent growth
days
D
no ATc
+ ATc
TATi/Δku80/
rTom7/Tom7wt
percent growth
days
E
days + ATc
0 1 2 3
1236
1048
720
480
242
146
66
anti-Tom40
F
1st Dimension: BN-PAGE
720
480
242
146
66
20
60
50
40
- ATc
day 2 + ATc
2nd Dimension:
SDS-PAGE

Supplemental Table S1. Summary of BLAST searches to identify mitochondrial import proteins in *T. gondii*.

S. cerevisiae	***A. thaliana***	***T. brucei***	***T. gondii***	E- value
TOM COMPLEX				
Tom40	*At*Tom40	None	TGME49_218280	3.0 x e^{-5}
Tom70	None	None	None[1]	N/A
Tom20	None	None	None	N/A
Tom22	*At*Tom22' (Tom9)	None	TGME49_255245	6.3 x e^{-4}
Tom5	None	None	None	N/A
Tom6	None	None	None	N/A
Tom7	*At*Tom7	None	None	N/A
None	*At*Tom6.0	None	None	N/A
None	*At*Tom6.3	None	None	N/A
None	*At*Tom20	None	None	N/A
None	None	Atom40	None	N/A
None	None	Atom69	None	N/A
None	None	Atom46	None	N/A
None	None	Atom36	None	N/A
None	None	Atom14	None	N/A
None	None	Atom12	None	N/A
None	None	Atom11	None	N/A
OUTER MEMBRANE INSERTASE				
Sam50	*At*Omp85	*Tb*Sam50	TGME49_205570[2]	5.0 x e^{-6}
Sam35	None	*Tb*Sam35?	None	N/A
Sam37	None	None	None	N/A
Mdm10	None	None	None	N/A

PRESEQUENCE TRANSLOCASE				
Tim23	*At*Tim23	None	TGME49_214150	2.4 x e^{-11}
Tim17	*At*Tim17	*Tb*Tim17	TGME49_312220	1.7 x e^{-33}
Tim50	*At*Tim50	None	TGME49_283590[3]	3.2 x e^{-11}
Tim21	None	None	None	N/A
Mgr2	None	None	TGME49_316140	1.2 x e^{-6}
PRESEQUENCE MOTOR				
mtHsp70	*At*mtHsp70	*Tg*mtHsp70	TGME49_251780	3.5 x e^{-209}
Mge1	*At*GrpE	*Tb*GrpE	TGME49_265220	4.5 x e^{-26}
Tim44	*At*Tim44	None	TGME49_227830	3.4 x e^{-9}
Pam18	*At*Pam18	*Tb*Pam18	TGME49_202810	9.9 x e^{-15}
Pam16	*At*Pam16	*Tb*Pam16	TGME49_249910	6.0 x e^{-6}
MIA COMPLEX				
Mia40	*At*Mia40	None	None	N/A
Erv1	*At*Erv1	*Tb*Erv1	TGME49_210787 TGME49_288620 TGME49_232815	5.0 x e^{-20} 2.5 x e^{-18} 1.1 x e^{-6}
TIM22 complex				
Tim22	*At*Tim22	None	TGME49_225710	7.3 x e^{-18}
Tim54	None	None	None	N/A
Tim18	None	None	None	N/A
Sdh3	*At*Sdh3	None	None	N/A
SMALL TIMS				
Tim8, Tim9, Tim10, Tim12, Tim13	*At*Tim8, *At*Tim9, *At*Tim10, *At*Tim13	*Tb*Tim9, *Tb*Tim10, *Tb*Tim8-like	TGME49_260850[4] TGME49_215390	1.7 x e^{-10} 2.8 x e^{-10}

			TGME49_227870 TGME49_254610 TGME49_274090	3.3 x e^{-7} 8.1 x e^{-4} 2.2 x e^{-2}
PRESEQUENCE PEPTIDASE and other peptidases				
Mpp-α	*At*Mpp-α	*Tb*Mpp-α	TGME49_202680	4.8 x e^{-54}
Mpp-β	*At*Mpp-β	*Tb*Mpp-β	TGME49_236210	2.1 x e^{-85}
Imp1	*At*Imp	*Tb*Imp	TGME49_268910	6.1 x e^{-15}
Oct1	*At*Oct1	*Tb*Oct1	TGME49_272670	2.2 x e^{-24}
Icp55	*At*Icp55	None	None	N/A
OXA1 insertase				
Oxa1	*At*Oxa1	*Tb*Oxa1	TGME49_312430[5]	4.3 x 10^{-4}

[1]Top hits are to Sti1-like proteins that contain tetratricopeptide repeat domains.

[2]Identified in BLAST searches using *At*Omp85 as a query.

[3]Note that this is not the top hit in the *T. gondii* genome against *Sc*Tim50, but is the only protein identified in reciprocal BLAST searches (i.e. whose top hit is to *Sc*Tim50 when querying the *S. cerevisiae* genome).

[4]BLAST scores based on searches using *Sc*Tim10 as a query.

[5]Identified in BLAST searches using *At*Oxa1 as a query.

The Import of Proteins into the Mitochondrion of Toxoplasma gondii

Giel G. van Dooren, Lee M. Yeoh, Boris Striepen and Geoffrey I. McFadden

J. Biol. Chem. published online July 25, 2016
